TAMPEREEN TEKNILLINEN YLIOPISTO
TAMPERE UNIVERSITY OF TECHNOLOGY

JUKKA VARJO

IMPLEMENTING A TEXTURE ANALYSIS SOFTWARE FRAME FOR MAGNETIC RESONANCE IMAGE DATA IN MATLAB

Master of Science Thesis

Examiner: Professor Hannu Eskola
Examiner and topic accepted by the Faculty of Computing and Electrical Engineering on November 7th, 2012

ABSTRACT

TAMPERE UNIVERSITY OF TECHNOLOGY
Master's Degree Programme in Electrical Engineering
VARJO, JUKKA: Implementing Texture Analysis Software Frame for Magnetic Resonance Image Data in MATLAB
Master of Science Thesis, 42 pages, 1 Appendix page
May 2014
Major: Medical Informatics
Examiners: Professor Hannu Eskola and Minna Sikiö (MSc)
Keywords: Texture analysis, magnetic resonance imaging, MaZda, MATLAB

This thesis was based on the need to develop a generic software application frame for texture analysis of magnetic resonance (MR) images. In collaboration with the research group at the department of Medical Imaging Centre and Hospital Pharmacy (MICHP) at Tampere University Hospital (TAUH) the goal was to improve the user experience and work flow as well as implement a completely new user interface and key functionalities. The platform was required to be complex enough to manage with image processing algorithms and to provide high level and easily modifiable software architecture. The research group having years of experience with an open-source texture analysis oriented MaZda software the focus of this thesis was to analyse and solve the restrictions based on the observations from using MaZda.

MATLAB was chosen as the programming platform due the high-level syntax with powerful built-in properties *e.g.* Image Processing Toolbox (IPT) that would allow proficient support for computationally demanding processes. Another advantage with MATLAB was the interface support for languages like Fortran, C and C++. MATLAB being commercial software platform, it was acknowledged that achieving a standalone end product would not be possible. Computational performance was also omitted for the purpose this thesis not only due to MATLAB's limitations but also to keep the scale contained.

The improvement suggestions provided by the research group were considered as a rough specification for the software to be implemented. These requirements included extensibility in terms of texture analysis algorithms and simplified user interface to improve the work flow. Selecting MATLAB as the programming environment extended the group of people capable of contributing to the tool in the future. Implementing the frame from the beginning allowed the texture analysis parameters and features to be fully configurable instead of static. The modular visual structure of the software allowed the user to switch between image sets more easily. Removing the region of interest (ROI) limitation ensured that same image set could be utilized more efficiently.

The implemented MATLAB application provides a basic frame for more convenient medical image processing flow for texture analysis of MR images but further testing and development is required to complement the tool.

TIIVISTELMÄ

TAMPEREEN TEKNILLINEN YLIOPISTO
Sähkötekniikan koulutusohjelma
VARJO, JUKKA: Magneettiresonanssikuvien tekstuurianalyysisovelluksen kehittäminen MATLAB-ympäristössä
Diplomityö, 42 sivua, 1 liitesivu
Toukokuu 2014
Pääaine: Lääketieteellinen informatiikka
Tarkastajat: professori Hannu Eskola ja Minna Sikiö (DI)
Avainsanat: Tekstuurianalyysi, magneettiresonanssikuvaus, MaZda, MATLAB

Tämän diplomityön tuloksena on toteutettu magneettiresonassikuvien tekstuurianalyysiin tarkoitettu käyttöliittymä yhteistyössä Tampereen yliopistollisen sairaalan kuvantamiskeskuksen tekstuurianalyysiin keskittyvän tutkimusryhmän kanssa. Työn tarkoituksena oli luoda laajennattavissa oleva ohjelman runko käytettävyyttä ja sujuvuutta korostaen. Luotavan ohjelma-alustan vaatimuksina esitettiin riittävä kompleksisuus kuvankäsittelytarkoitukseen soveltumiseksi sekä korkean tason muokattavuusmahdollisuuksia tarjoava arkkitehtuuri. Tutkimusryhmän vuosien kokemus avoimen lähdekoodin tekstuurianalyysiin tarkoitetusta MaZda-sovelluksesta oli perustana havaittujen rajoitusten ja puutteiden analysoimisessa ohjelmarungon toteuttamisvaiheessa.

MATLAB-ohjelmisto valittiin sovelluksen kehitysalustaksi korkean tason syntaksin ja monipuolisten sekä tehokkaiden sisäänrakennettujen työkalujen, kuten esimerkiksi Image Processing Toolboxin, ansiosta. Tämä kuvankäsittelyyn tarkoitettu MATLAB-ohjelmiston laajennus mahdollisti tarvittavien laskennallisesti vaativien prosessien suorittamisen. Lisäksi ohjelmisto tarjoaa rajapinnan, jonka avulla C ja C++ sekä Fortran –kielillä toteutettua olemassaolevaa koodia voidaan hyödyntää. MATLAB-ohjelmiston kaupallisuus huomioitiin suunnitteluvaiheessa ja luotavan ohjelman käytön rajoittaminen MATLAB-ympäristöön katsottiin olevan hyväksyttävää. Ohjelmakoodin laskennalliseen tehokkuuteen ei työssä kiinnitetty erityistä huomiota vaan pääpaino pidettiin käyttöliittymän suunnittelussa, magneettiresonanssikuvien visualisoinnissa sekä ROI-alueiden piirtämisen ja tekstuuriparametrien laskennan toteuttamisessa.

Käyttöliittymän toteutus tehtiin tutkijaryhmän parannusehdotusten pohjalta. Ehdotukset toimivat suuntaa-antavana määrittelydokumentaationa sisältäen vaatimukset tektuurianalyysialgoritmien laajennettavuudesta ja helppokäyttöisestä käyttöliittymästä. MATLAB-ohjelmiston valinnan toteutusalustaksi katsottiin antavan hyvät mahdollisuudet sovelluksen jatkokehityksen kannalta. Toteuttamalla tekstuurinanalyysiohjelma alusta alkaen pystyttiin täysin kontrolloimaan toteutettavia ominaisuuksia. Ohjelman käyttöliittymän modulaarinen rakenne mahdollistaa esimerkiksi käyttäjän vaivattoman siirtymisen usean kuvasarjan välillä. Lisäksi ROI-alueiden MaZda-sovelluksessa havaitut puutteet, kuten 16 alueen maksimirajoitus, onnistuttiin poistamaan ja samalla lisäämään analyysiprosessin sujuvuutta.

Toteutettu MATLAB-pohjainen tekstuurianalyysiin suunnattu käyttöliittymä tarjoaa perustan käyttäjäystävällisemmälle lääketieteellisten kuvien käsittelylle keskittyen magneettiresonanssikuvien tekstuurianalyysiin. Sovelluksen jatkokehityksen kannalta on tärkeää suorittaa hyväksymistestaus loppukäyttäjillä ennen varsinaista käyttöönottoa ja valvoa lisätoiminnallisuuksien toteutusta.

PREFACE

This thesis was completed for the Medical Imaging Centre and Hospital Pharmacy at the Department of Radiology of Tampere University Hospital in collaboration with the Department of Biomedical Engineering of Tampere University of Technology.

I want to express my most sincere gratitude to my examiners Professor Hannu Eskola (PhD) and Minna Sikiö (MSc) for guidance and patience. I am also most grateful for Prasun Dastidar (MD, PhD) for arranging the funding and Baran Aydogan (PhD) for providing technical support with MATLAB.

I would also like to express my gratitude to the texture analysis research group members Kirsi Holli (PhD), Maija Rossi (PhD), and Sami Savio (MSc) for their insight and assistance.

Special thanks go to my beloved partner Emma Luukka who kept on believing in me through thick and thin and to my family for life-long caring.

Helsinki, May 2014

Jukka Varjo

TABLE OF CONTENTS

LIST OF SYMBOLS AND ACRONYMS

AD	Alzheimer's disease
ADC	Apparent diffusion coefficient
API	Application programming interface
ASM	Angular second-moment
BMRI	Breast magnetic resonance imaging
BOLD	Blood oxygenation level dependent
CAD	Computer-aided diagnosis
CT	Computed tomography
DCE-MRI	Dynamic contrast enhanced magnetic resonance imaging
DICOM	Digital imaging and communications in medicine
dMRI	Diffusion magnetic resonance imaging
DTI	Diffusion tensor imaging
DWI	Diffusion-weighted imaging
DWT	Discrete wavelet transform
EEG	Electroencephalogram
FID	Free induction decay
FLAIR	Fluid-attenuated inversion recovery
FLASH	Fast low angle shot
fMRI	Functional magnetic resonance imaging
FOV	Field of view
GLCM	Grey-level co-occurrence matrix
GRE	Gradient echo
GUI	Graphical user interface
GUIDE	Graphical User Interface Layout Editor
HD	Huntington's disease
IPT	Image Processing Toolbox
IR	Inversion recovery
ITK	Insight Toolkit
JIT	Just-in-time
JME	Juvenile myoclonic epilepsy
k-NN	k-nearest neighbour

LBP	Local binary pattern
MEDIC	Multi echo data image combination
MICHP	Medical Imaging Centre and Hospital Pharmacy
MIPAV	Medical Image Processing, Analysis and Visualization
MIT	Massachusetts Institute of Technology
MITK	Medical Imaging Interaction Toolkit
MMSE	Mini-mental state examination
MR	Magnetic resonance
MRA	Magnetic resonance angiography
MRI	Magnetic resonance imaging
MRS	Magnetic resonance spectroscopy
MTBI	Mild traumatic brain injury
NDA	Nonlinear discriminant analysis
NHL	Non-Hodgkin’s lymphoma
NIH	National Institutes of Health
NLM	National Library of Medicine
NMR	Nuclear magnetic resonance
OSI	Open Systems Interconnection
PACS	Picture archiving and communication system
PCA	Principal component analysis
PD	Parkinson's disease
PVE	Partial volume effect
ROI	Region of interest
SNR	Signal-to-noise ratio
SPL	Surgical planning lab
SPSS	Statistical Package for the Social Sciences
SQuaRE	Quality Requirements and Evaluation
STIR	Short T_1 inversion recovery
T_1	Longitudinal relaxation time
T_2	Transverse relaxation time
T_{2*}	T_{2*}-relaxation time
TAUH	Tampere University Hospital
TE	Echo time
TR	Repetition time

TRE	Tumour response evaluation
VOI	Volume of interest
VTK	Visualization Toolkit
2D	Two-dimensional
3D	Three-dimensional
4D	Four-dimensional

1 INTRODUCTION

Medical imaging modalities have evolved with increasing pace in recent years. Technological innovations regarding the healthcare sector may seem slow compared to modern consumer devices, but reforming an entire diagnostic process from image acquisition to computational image analysis requires the input of thousands of researches from hundreds of areas of expertise.

Today high resolution medical images provide more data than the human perception can process and detecting even the slightest changes may have a significant meaning in early anticipatory diagnosis [1]. Long-term follow-up cancer treatments is one example where texture analysis could provide a computational approach for medical image evaluation based on mathematical interpretation of image data. Although clinical applications and complete automation is still some years away, decision support for diagnosis is one of the key applications of texture analysis methods today.

Two-dimensional (2D) slices are the most common types of medical images and they can be effectively converted into three-dimensional (3D) image sets respectively. Texture analysis methods are a common tool in aiding magnetic resonance imaging (MRI) interpretation for more accurate diagnosis both in two and three dimensions. MRI produces a high resolution image with clear tissue contrast. In order to extract maximum amount of data from the medical image acquisition systems various computational methods have been developed. MaZda software is one example of such method being able to extract hundreds of texture analysis parameters [2]. However, processing and storing this data conveniently results in a completely new range of challenges.

The aim of this thesis is to provide an extendable custom software frame for texture analysis of magnetic resonance (MR) images using MATLAB environment. In collaboration with the texture analysis research group at the Medical Imaging Centre and Hospital Pharmacy (MICHP) of Tampere University Hospital (TAUH) the issues with current texture analysis methods and tools are addressed.

This thesis is divided into six chapters. In Chapter 2 the theories behind MRI and texture analysis of medical images are presented in more detail for further understanding the image processing steps coming up later in the thesis. Recent research results by TAUH texture analysis research group and the most prominent open-source applications are also introduced including the MaZda software. In addition an overview on software development in medical informatics is presented. Chapter 3 investigates the features of MaZda and introduces the MATLAB programming environment. The software development process from requirements to design is explained and illustrated.

The requirements for the initial software frame implementation are also presented. Chapter 4 introduces the results of the implemented software frame and the adapted functionality presenting the software architecture as well as the user interface modules individually. Chapter 5 discusses the practicality and the implementation process by presenting the detected benefits and disadvantages in texture analysis of MR images and in medical imaging in general. Finally the thesis is concluded in Chapter 6 with an overview on the topic.

2 BACKGROUND

Medical imaging field has gone through a massive transformation during the last decades and this evolution shows no sign of slowing down. Starting from the early 1900's with the discovery of X-ray beams by Professor Röntgen and slowly moving on to nuclear medicine, ultrasound scanning and eventually leading to various digital imaging techniques such as computed tomography (CT) and MRI, the path to modern day imaging devices has been extraordinary. Especially the rapid development of personal computers has enhanced both the image acquisition process as well as the diagnosis through numerous post-processing features. The increasing amount of data is yet to be fully utilized which calls for further improving the analysis of medical images ultimately leading to new computer-aided diagnosis (CAD) systems.

This thesis will focus on texture analysis of MR images and medical image processing software. Other imaging modalities are not explained in detail regardless that analogous methods can be utilized for most of the digitalized imaging systems available. Texture analysis methods are discussed thoroughly as well as the MaZda software features. Other open-source image processing software are shortly revised as a reference for the MATLAB implementation process introduced later on.

Recent studies conducted by the research group were analysed in order to discover how MaZda had been previously utilized in texture analysis purposes. Six different medical disorders researched by the group at TAUH are reviewed in Chapter 2.4 and latest MaZda related research from international groups are introduced in Chapter 2.5.

2.1 MRI

MRI has been the standard non-invasive, non-ionising modality of medical practice for decades despite its relatively short history. The discovery of MR phenomenon in 1946 was followed by a period of molecular analysis using nuclear magnetic resonance (NMR) for the first time [3]. In 1971 Raymond Damadian introduced a more medical approach for revealing the different relaxation times of healthy tissue and tumor [4]. This revolutionary discovery is still considered the core aim in most cancer imaging cases. The early image acquisition process was slow and expensive but both aspects were successfully reduced during the following decades. Replacing often painful invasive examinations, improving cancer diagnostics and evolving from tomographic to genuine 3D anatomical imaging modality to aid in preoperative procedures are just a few examples of the pioneer advancements virtue to MRI. Several Nobel prizes have been awarded honouring the people involved in the critical stages of developing the MRI modality.

During the years MRI has evolved into a multidimensional family of techniques. For example the quality of MR images can be enhanced by a broad spectrum of contrast mechanisms. This is a prime example of the flexibility of MRI. More detailed discussion of the sub-modalities is presented in Chapter 2.1.2.
Despite the abundance of parameters involved in MRI the resulting image is largely characterized by a relatively small set of parameters namely repetition time (TR), echo time (TE), slice thickness, field of view (FOV) and matrix size. TR and TE affect most on image contrast whereas the resolution is defined by the combination of slice thickness, FOV and matrix size. [5]

Based on the MR of hydrogen nuclei frequency response MRI excels in imaging materials that contain water and fat e.g. tissue and human body in general. Introducing energy to the system by adjusting the external radio frequency the electrical signals irradiated during the proton spin relaxation can be measured. The frequency caused by the precession is known as Larmor frequency ω_0 which is characteristic to each nuclei with different gyromagnetic ratio γ and the dominant magnetic field strength β_0.

$$\omega_0 = \beta_0 \gamma \tag{2.1}$$

The relaxation times are called spin-lattice relaxation time (T_1) and spin-spin relaxation time (T_2) respectively. T_2 can also be noted by T_{2*} meaning that the combined time constant of molecular interaction and magnetic field variation effects have been taken into consideration. T_1 expresses the time constant of longitudinal magnetization precession to its equilibrium and T_2 describes the time constant of transverse magnetization precession respectively. The relaxation times are affected by the TR and TE parameters. High T_1 contrast can be generated by long TR and short TE and high T_2 contrast is achieved with long TR and long TE. [3; 5]

2.1.1 Imaging sequences

The possibility to modify the MRI process allows specified applications of this powerful modality to be created. Generally NMR signals can be either free induction decay (FID) or spin echo (SE) type. The imaging sequences are categorised into families of spin echo, inversion recovery (IR) and gradient echo (GRE) sequences. [5]

SE technique is the fundamental imaging sequence used in clinical diagnosis. SE signal is produced by 90° and 180° radio frequency pulses. Gradient coils are also used in three dimensions for increased signal location accuracy. Decent contrast and minimal artefacts make SE a reliable pulse sequence. [5]

IR sequence is similar to SE but with an added 180° pulse. Sending the inversion pulse in the beginning of the sequence results in spins aligning to the magnetic field inverted *i.e.* anti-aligned. Two most common IR sequences are fluid-attenuated IR (FLAIR) and short T_1 IR (STIR). [5]

GRE techniques are regarded as the simplest type of imaging sequence and they are based on FID and a radio frequency pulse between 0° and 90°. The flip angle without a

180° pulse is used for the spins to be in phase only at the centre of the sequence so that the reversal of the gradient results in the echo. Applying GRE techniques results in shorter TE and TR times which decrease the required overall imaging time. [3]

2.1.2 Imaging techniques

In addition to flexible imaging sequences a variety of characteristic MRI techniques have evolved into a group of medical imaging sub-modalities. Deviating from the static imaging modalities of MRI the functional MRI (fMRI) was develop for detecting and registering brain activity caused by external stimuli. Combined with the blood oxygenation level dependent (BOLD) contrast imaging method the neural activity of the brain can be visualized. This is possible due to the minor differences in ratios of oxyhemoglobin and deoxyhemoglobin also referenced as the hemodynamic response that coincides with the brain being excited. [6]

Another specific branch of imaging modalities are the diffusion MRI techniques. The diffusion process of mainly water molecules is utilized and the measured signal is mapped and characterized in 3D as a function of spatial location in diffusion-weighted imaging (DWI) and in diffusion tensor imaging (DTI) which is considered a sub-modality of DWI. From these diffusion patterns the tissue characteristics can be observed. The diffusion anisotropy degree, magnitude and orientation is described by the diffusion tensor. [7; 8]

Four-dimensional (4D) imaging adds a temporal dimension in addition to three spatial dimension provided by standard MRI. Magnetic resonance angiography (MRA) can employ the time component in imaging the blood flow in blood vessels. In addition with dynamic contrast-enhanced MRI (DCE-MRI) the 4D image data has been utilized in breast lesion analysis. [9]

The strength of the magnetic field in MRI is reflected directly to the spatial resolution of the acquired image. For imaging the neurobiological and neurochemical processes in the brain the highest possible spatial resolution is required. The standard MRI device having usually 1.5T magnetic field and 3.0T devices slowly becoming more common, the ultrahigh field MRI device with magnetic field of 7T has been used for Huntington's disease (HD) patient imaging [10]. One technique that has benefited from 3T devices becoming increasingly common is the magnetic resonance spectroscopy (MRS) which provides means for analytical approach for detecting the chemical content of the object. [11]

2.1.3 Artefacts

Being a highly sensitive imaging system, MRI is also prone to various types of artefacts from different origins. Artefacts are considered unintended features on the resulting image that are not present in the object of interest. Noise related artefacts are relatively easy to cancel with appropriate filtering or shielding of the imaging unit. Magnetic field inhomogeneity, damaged gradient coil and paramagnetic object near the magnetic field

may also result in spatial distortion or artefacts. Some imaging system related artefact correction methods are discussed in Chapter 2.2.6. Motion artefacts are caused by the movement of the object that is being imaged. The long imaging sequences of MRI are extremely sensitive to detect even the slightest changes in patient posture and this may result in false alignment of the images. Involuntary physiological functions such as the beating of the heart muscle, flowing of blood and the thorax movement caused by inhaling and exhaling cannot be shut down, but fastening and supporting the area of interest may prevent most of the motion artefacts. Until the spatial resolution of MRI is increased, partial volume effect (PVE) remains one source for possible artefacts. Often the anatomical structure of interest to be imaged is smaller than the image voxel resulting in weighted average of two different tissue types to be detected instead of discriminating them. Reducing the pixel and voxel size with lower slice thickness and higher magnetic fields may result in decrease in signal-to-noise ratio (SNR). [3]

Data collection process of all multi-parameter imaging techniques may degrade the quantification results. Carefully addressing all the possible sources of image artefacts before and during the image acquisition process is critical in providing the cleanest, most reliable data for the processing and analysing techniques to base upon.

2.2 Texture analysis

Early stages of modern day texture analysis was first experimented with aerial photographs and later with satellite images taken by the probes on the orbit in the 1950s [12]. Defining the features that characterize textural differences was taken a special interest in after the digital revolution of personal computers and digital cameras occurred. This search for meaningful parameters is still the underlying inspiration for textural analysis research of images. [13]

Textures can be perceived as sub-patterns of an image but the very concept of texture has subjectivity to it and no unambiguous description is known. Texture can be regarded as any complex visual pattern or sub-pattern of different brightness, colour, shape or size. [1; 14]

2.2.1 Structural approach

The textures containing distinct structures or geometrical properties are best analysed by the structural approach. The human vision is effective in perceiving these regular and periodic shapes and textures. This makes structural approach useful in pattern recognition but not quite optimal for textural analysis of medical images due to their random and non-homogeneous features. [15]

2.2.2 Model-based approach

Texture analysis can also be based on sophisticated mathematical models such as fractal or stochastic models. Interpretation of the image texture is achieved by estimating the

model parameters and then applying these values to the actual texture analysis. The main disadvantage of the approach is the high computational complexity, but it has been successfully utilized in segmentation purposes using for example the autoregressive (AR) model features. Causal AR of the image f_s can be calculated if noise e_s, neighbourhood N_s and model parameter vector Θ_r are known: [5; 14]

$$f_s = \sum_{r \in N_s} \theta_r f_r + e_s \tag{2.2}$$

For the AR model discrimination of shapes within the image is quintessential. The model-based methods are in essence mimicking the texture so that recreating the pixel value comes as close to the original as possible. [14]

2.2.3 Transform approach

The time-frequency domain is utilized in texture analysis by the Gabor functions and wavelet transform by both resorting in the Fourier transform. Unlike Fourier functions wavelet functions are localized in space which makes them feasible for texture analysis. [16; 17]. Performing frequency analysis on texture introduces a completely different feature set compared to any other approach. The wavelet transform is calculated by decomposing the image by dilation and translation to a set of wavelet functions and a "mother" wavelet. Applying this process discretely results in discrete wavelet transform (DWT). The basis wavelet function is defined by

$$\theta_{s,l}(x) = 2^{-s/2}\theta(2^{-s}x - 1) \tag{2.3}$$

where parameters scale s and dilation l are known [17]. Combined with scaling and computational simplicity owing to the transformation to frequency domain wavelets offer a discrete option to the continuous Gabor transform in texture feature classification. [18]

2.2.4 Statistical approach

The stochastic nature of quantitative texture analysis makes it suitable for statistical methods. These methods utilize spatial distribution of grey-scale values of each signal represented by the pixel or voxel. Statistically derived features can be based on histogram, absolute gradient, run-length matrix or co-occurrence matrix.

Histogram features derive from the spatial grey value intensity distribution of the image. Each pixel is categorized according to the value. The histogram range depends on the pixel value range which correspondingly is determined by the image bit value. Mean, variance, skewness and kurtosis are examples of parameters that can be calculated using the histogram of the image. [14]

Absolute gradient describes the spatial variation of the image by detecting sudden intensity value changes between the pixel of interest and the neighbouring pixels. The size of the neighbourhood can vary but increasing it too much will result in reduced computational performance. The value of gradient is high for neighbouring pixels that have very distinct values and low if the difference in pixel values is minimal. The gradient can be either negative or positive depending on the value change sign. However, it is common to use the absolute value for image processing purposes. Similarly to histogram-based parameters mean, variance, skewness and kurtosis can be also calculated for the absolute gradient. [14]

Run-length matrix is used for detecting subsequent pixel values or runs of pixels from an image. The number of consecutive pixel values to be searched and the direction of the search can be adjusted. Horizontal, vertical and the two diagonal directions are commonly used for directions resulting in four result matrices. Parameters like short run and long run emphasis moments, grey level nonuniformity and run-length nonuniformity can be derived using the run-length matrix. [14]

The joint probability distributions of pairs of pixels is called the co-occurrence matrix. This method is widely used in quantitative texture analysis. The second order histogram of the intensity values of the image provides the count of pixel pairs (i,j) of distance d apart along the direction Θ in a matrix $h_{d\Theta}(i,j)$. Representation of co-occurrence matrix using 0° direction is depicted in Figure 2.1 with 3x3 image matrix resulting in 8x8 co-occurrence matrix due to the highest intensity value of eight.

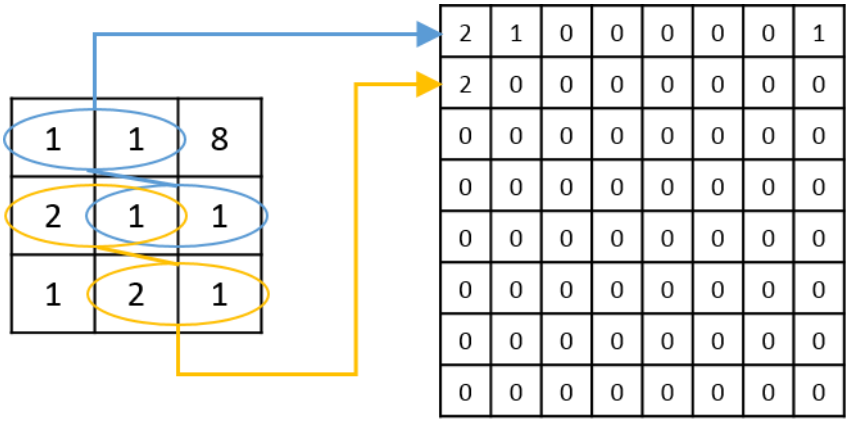

Figure 2.1. *8x8 co-occurrence matrix created based on 3x3 image matrix.*

By dividing this element by the total number of pairs R in the image a joint probability of two pixels is achieved noted as $p_{d\Theta}(i,j)$. The resulting matrix dimension is equal to the number of intensity values for each distance and direction respectively thus only short distances and limited amount of angles are commonly used. [5]

The co-occurrence matrix is the basis of several different textural features such as angular second-moment (ASM), contrast, correlation, sum of squares, variance, inverse moment, entropy and different types of average values. ASM describes the homogeneity of the image producing low values for highly homogenous texture and low values for inhomogeneous textures. Contrast is calculated using the difference moment of the co-

occurrence matrix and it represents the amount of local variations in the image. Greater total difference between the grey-values in an image result in higher contrast. The linear-dependencies between the grey-level values are measured as the correlation. Images with similar intensities on large areas result in high correlation values. Sum of squares is also known as the energy or variance. Like the co-occurrence matrix itself the features derived from it are also dependent on the distance and direction used in the original co-occurrence matrix calculation. [13]

2.2.5 Local binary patterns

Local binary patterns (LBPs) are based on the texture spectrum model and provide an additional statistical approach to texture analysis. In the texture spectrum model a concept of texture unit is proposed. The texture unit is defined for each pixel value by the eight neighbouring pixels values in a 3x3 matrix. Each neighbouring pixel is compared to the central pixel and assigned a texture unit value accordingly. Neighbouring intensities with lower values compared to the reference pixel are marked with 0, intensity values equal to the reference pixel are marked with 1 and intensity values with higher values are marked with 2. The texture unit number is read starting from upper left corner of the newly calculated 3x3 matrix proceeding clockwise. Eight elements with three possible values results in 6561 different texture unit combinations. These combinations are labelled as a single value called the texture unit number N_{TU} according to

$$N_{TU} = \sum_{i=1}^{8} E_i \cdot 3^{i-1} \qquad (2.4)$$

where *Ei* is the texture unit value. [19; 20]

LBPs refine the concept of texture units by narrowing the possible combinations down to 256. This is achieved by assigning only binary values when comparing the neighbouring pixel to the reference pixel which is analogous to thresholding. In LBPs the neighbouring intensities with lower values compared to the reference pixel are marked with 0 and intensity values equal to or greater than the reference pixel are marked with 1. For the classical LBP operator additional labelling is not required because a binary value (*i.e.* eigenvalue) is created when reading the values from the 3x3 matrix as depicted in Figure 2.2.

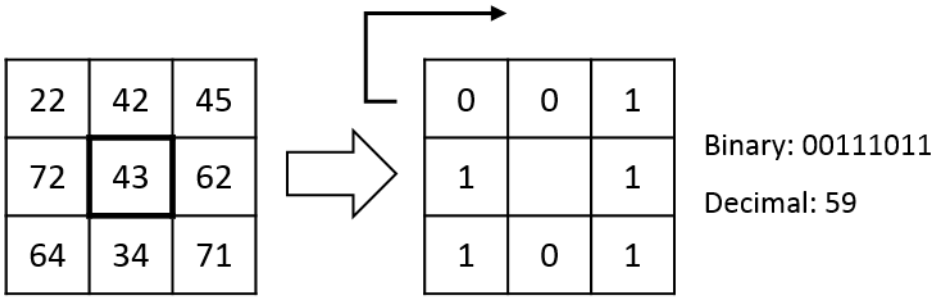

Figure 2.2. *Illustration of the classical 3x3 neighbourhood LBP operator.*

The neighbouring pixels are also be weighted by multiplying the binary matrix by a weight matrix and summing the values results in a characteristic LBP number. This grey-scale invariant and computationally low complexity method was originally introduced by Ojala, Pietikäinen and Harwood in 1994. [21-23]

Early solutions for rotation invariance of LBP were based on using a limited subset of uniform patterns. By bitwise shifting the LBP value a corresponding angle of rotation can be found. As a result two rotation-invariant LBP operators known as LBP_8^{riu2} and LBP_{16}^{riu2} and two rotation-invariant variance measures VAR_8 and VAR_{16} were introduced for 3x3 and 5x5 neighbourhoods respectively [24]. Further improvement of multi-resolution grey-scale and rotation invariant texture classification methods is known as $LBP_{P,R}^{riu2}$ operator [25; 26].

Textural information extracted using LBP has been introduced by Ahonen *et al.* for automated face recognition and description purposes. Several local descriptions of the face were constructed and then combined into a global description for obtaining an improved feature vector. [27; 28]

The rotation-invariant LBP has been reported with two primary weak points. By merging all non-uniform patterns into one pattern a significant amount of texture data is lost. The loss is emphasized with increased neighbourhood. The stochastic components of the texture are also submitted to the effects of more regular and structural components. Rotation-invariant LBP operators are also sensitive to noise because the local pattern label changes easily. The extended LBP utilizes the non-uniform local patterns to classify the characteristic structural properties and it was discovered to outperform the classical rotation-invariant LBP with higher tolerance to noise in larger neighbourhoods. [29]

Another similar approach in developing a LBP robust to noise involved eliminating the bit values affected by noise from the binary matrix to produce more regular patterns. The elimination was done by a suitable circular majority voting filter followed by labelling the local patterns that share both bitwise transition and the count of true value bits. [30]

The conventional approach of LBP in 2D with various improvements and enhancements has established a strong position in image texture classification but not many 3D extensions have been developed. The main complexity of employing a LBP in 3D space is achieving the rotation invariance. The three degrees of freedom result in

great number of possible rotation directions. By applying spherical harmonics with fast correlation computational challenges were somewhat contained. Evaluating the performance on 3D image data by cell nuclei classification the 3D LBP resulted in slightly improved accuracy compared to uniform LBP but the cost of computational complexity was still regarded as major disadvantage. [31]

2.2.6 Texture analysis of MR images

MRI provides high quality image data that can be readily analysed by a multitude of computational methods. The quantitative texture analysis process of medical images can be divided into three stages: feature extraction, texture classification and texture segmentation. Having completed the image acquisition process the first step is to define ways to compute texture parameters that numerically present the properties of the image texture. This often involves defining an area of interest for which the analysis is performed. Drawing the region of interest (ROI) areas in 2D and volume of interest (VOI) areas in 3D enables focusing the analysis on a confined area or volume because the assumption is often made, that within the ROI/VOI borders the texture is uniform and ideally consists of single type of tissue. [5]

The process of assigning an observation to a class from a predetermined set of classes is called classification hence being the central tool for of decision making. In texture classification the observation is substituted as the extracted texture feature parameter that is assigned to either healthy class or to pathological class. Classification is based on linear or nonlinear mathematical classifiers. The classifiers are adjusted by setting weight parameters and by training. A training data set is obtained from the observations with labelled information of the classes. The labelling is a confirmation of correct classification and is only done by a trained medical professional. From the classification errors made in training the classifier learns from these mistakes and adjusts the weights accordingly. [5]

Segmentation is the process of partitioning the image data according to the context into non-overlapping regions with high homogeneity and high correspondence to the object that was imaged. Segmentation can be done manually by a radiologist but sophisticated automated software have been developed to make the process faster. [5]

Promising, and often more common to traditional image processing field, techniques for texture analysis and classification are constantly being introduced to medical imaging applications. LBP methods described in Chapter 2.2.5 have recently been experimented with MRI texture identification. Inspired by the achievements in computer vision and face recognition, a robust rotation-invariant LBP operator was used for pre-processing image data. Even the slightest intensity inhomogeneity and nonuniformity of the original MRI data may result in drastic errors further along the computational analysis process albeit having no effect on visual diagnosis. Another hypothesis was that with an operator invariant to rotation the spatial alignment issues caused by patient movement could be addressed. For the experiment a group of bias fields of three with three

different intensity variation patterns were created to simulate MR image data inhomogeneity. Robustness of the LBP operator to bias fields and to discrete rotation steps of up to 60° in counter clockwise and clockwise directions were measured. Despite an increase was detected in LBP feature values for bias field the highest measured dissimilarity recorded was 0.04%. In rotation testing the LBP features decreased with more complex interpolation and higher LBP operator radius resulting in a robust outcome. Rotation-invariant LBP was successfully applied to MR images with artefacts and the method solved some of the inherent intensity variation and spatial misalignment problems of MRI. [32]

One distinct application of LBP related to medical image textures that has been studied in the field of MRI is image search and retrieval. As described earlier, the amount of medical image data increases with higher quality modalities becoming increasingly universal. To help finding relevant slices of MR images with specific pathological qualities can be essential to diagnostic purposes providing reference and inter-patient comparison in decision making process. Based on either texture or intensity features four techniques for image retrieval were introduced by Unay and Ekin in 2008 [32]. Pre-processing steps of alignment correction, intensity normalization and segmentation of the brain MR images to contain only tissue were required. LBP was selected for texture-based feature characterization whereas intensity distribution was observed using histogram only. With a grid consisting of 12 angular and 4 annular regions a spatial context factor was applied to both techniques to obtain optimal discrimination. Retrieval method based on texture features with added spatial context surpassed other combinations and resulted in best accuracy and speed in finding corresponding images from the data set. With promising results the implementation is yet to be introduced to a larger data set using unregistered data. [33]

Instead of selecting MR images from a database using texture related criteria, one approach utilizing LBP is the automated artefact detection. Especially DWI has been reported irreversibly suffering from motion artefacts. This is common with other MRI techniques as well in case the patient is an infant or an adult with a neurodegenerative disorder. Rejecting corrupted images and outliers prior to tensor estimation contributes to better quality DWI data. Disregarding the entire motion-corrupted DWI data set may be avoided by carefully evaluating the robustness of tensor estimation. A modified LBP with adaptive weighing was applied and a custom ranking system was used to identify image regions of different importance. This process enabled assessing texture in various spatial scales by interpolating grey-scale values in circular neighbourhoods. The ranking was done with 2D partial least squares enabling local textural features to be extracted for detecting artefacts from the DWI data set. The algorithm was applied prior to tension estimation as a pre-processing step which allowed compatibility with DTI analysis software regardless of type. As a result the slice-based identification excelled voxel-based identification in accuracy and the corrupted images were successfully rejected from the DWI data set preventing erroneous tensor estimation. [34]

2.3 Medical image processing software

Software engineering has not only impacted medical image acquisition but also the processing of the raw image data. This is best depicted by the abundance of available computer-based applications for specific prognostic and diagnostic purposes. While companies involved in producing medical imaging hardware often provide an integrated system with low level image processing software, there are several open-source products available for research and private use alike. Five of these systems with characteristic functional purpose and features are introduced to provide perspective into a multitude of medical imaging challenges and opportunities and a review of the outcomes that have been achieved.

2.3.1 Insight Toolkit variants

The Insight Toolkit (ITK) library is a standalone toolkit dedicated to the registration and segmentation of image data. The ITK launch was supported by National Institutes of Health (NIH) between 1999 and 2002 which was followed by the first official public release followed by funding for maintenance by the US National Library of Medicine (NLM). [35]

ITK-SNAP (also referred as SNAP) is an application for semi-automated active contour segmentation of medical images in 3D [36]. The name of the application reveals that it consists of two parts which can be considered as separate entities. Segmentation of medical images at the time was done by manually delineating the area of interest. The long time required for this process as well as the lack of 3D feedback inspired the developers to aim for automation. The traditional method in manual segmentation resulted often in error due to mismatches between subsequent slices. ITK-SNAP was released in 2004 providing both manual and semi-automatic 3D segmentation tools for different imaging modalities and computing platforms. The workflow of image segmentation involved three stages. After selecting the preferable method of contour propagation the user is required to initialize seed regions to the image for the active contour to evolve from. For the final stage partial differentiation equation weights for the active contour evolution needs to be entered. The novel user-guided approach offered excellent reliability in caudate nucleus validation tests in comparison with highly trained professionals. [36]

Another ITK-based software available is the Medical Imaging Interaction Toolkit (MITK) which combines the ITK and Visualization Toolkit (VTK) libraries. Developed by the Division of Medical and Biological Informatics at the German Cancer Research Center in Heidelberg the MITK extends the combination of ITK algorithms and VTK visualization with the support for complex user interface interactions. [37]

2.3.2 3D Slicer

Based on the Slicer software developed by the research groups at Massachusetts Institute of Technology (MIT) and Surgical Planning Lab (SPL) in 1999, 3D Slicer a widely used tool for quantitative image computing research. With the support of NIH 3D Slicer is being continuously improved and maintained. By the initiative of National Cancer Institute of the United States of America a Quantitative Imaging Network project was launched in 2008 heavily involving the use of 3D Slicer. The "ecosystem" of the software is described in Figure 2.3 which reveals that the ITK and VTK libraries discussed earlier is one of the key dependencies of 3D Slicer. [38]

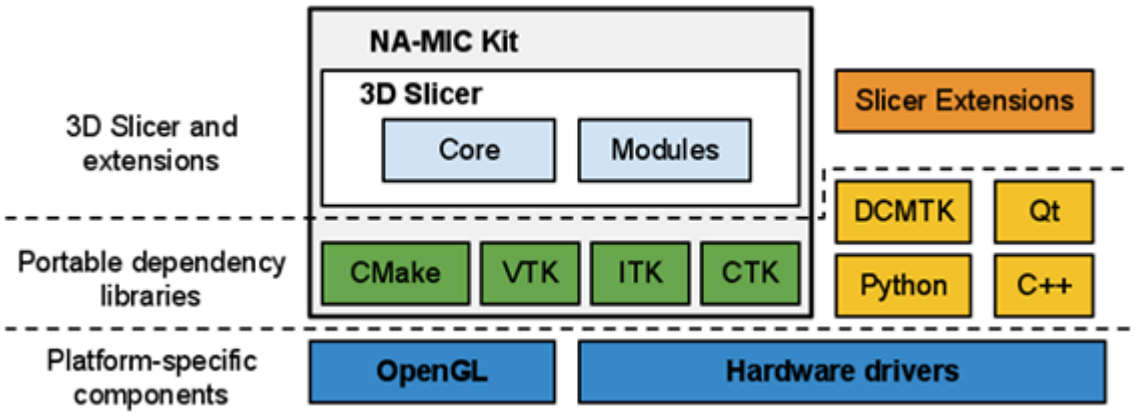

Figure 2.3. *3D Slicer software application architecture [38].*

3D Slicer itself consists of the core, modules and extensions and features a comprehensive selection of functionalities, portability across most common computing platforms with profuse support for extensibility.

2.3.3 ImageJ

Not only for medical imaging purposes but for scientific image processing purposes in general one software has managed to evolve through a respectable lifespan of almost three decades. Originating from the 1987 NIH Image by Wayne Rasband the ImageJ software, as it is called since 1997, provides a range of image processing features achieved by the community-driven development model. This model consisted of four principles on how additional functionality could be embedded to the software or how existing features are to be enhanced. First method was a direct contact with Rasband himself concerning the suggestion. The second approach was to seek approval of another member of the community. The third way was to implement a solution and then sharing it with the community. The final method was to give feedback on an existing feature. With such a general approach today ImageJ supports several hundred plugins and macros as well as connections to third-party software such as MATLAB. This level of integration ability has generated a number of variants of the original ImageJ software focusing on microscopic imaging, astronomy or biology related research. [39]

2.3.4 MIPAV

The MIPAV (Medical Image Processing, Analysis and Visualization) software was launched in 2000 by NIH at the Center for Information Technology in Maryland (US) and provides quantitative analysis and visualisation of medical images. MIPAV is implemented in Java language and supports multiple computational platforms and imaging modalities. The tool is mainly aimed for the researchers at NIH but is freely available. MIPAV also provides an application programming interface (API) which can be used for more customized analysis. For the NIH researcher the possibility of direct access to a DICOM server for patient data and image retrieval using picture archiving and communication system (PACS) is also available. MIPAV can be extended by Java plugins for more specific research purposes. [40; 41]

2.3.5 MaZda

Named after the Polish word for 'co-occurrence matrix' (Macierz Zdarzen) the MaZda program has been under developement since 1998. The software application was created at the Institue of Electronics of the Technical University of Lodz in Poland for quantitative texture analysis of medical images. MaZda was created as part of the European COST B11 "Quantitative Analysis of Magnetic Resonance Image Texture" project in 1996 and it is based on the German NMRWin program originally designed for texture analysis of mammogram images. The early studies involved automated texture analysis using NMRWin software application on axial images of dystrophic thigh muscle tissue in 1999. Muscle was selected for having a longitudinal structure thus PVE could be minimized. The sufficient distance from involuntary physiological signal sources that are subject to causing artefacts allowed higher quality images to be obtained. In addition the axial slices provide a variety of muscle groups that can be observed visually. Most of the fundamental functionality of NMRWin passed on to MaZda but several improvements were also made one being the enhanced graphical user interface (GUI) depicted in Figure 2.4. With the stable update rate the software was developed with, MaZda is considered the successor of the first originally texture analysis oriented software and even today remains in active use since an application with superior features is yet to emerge. [42-45]

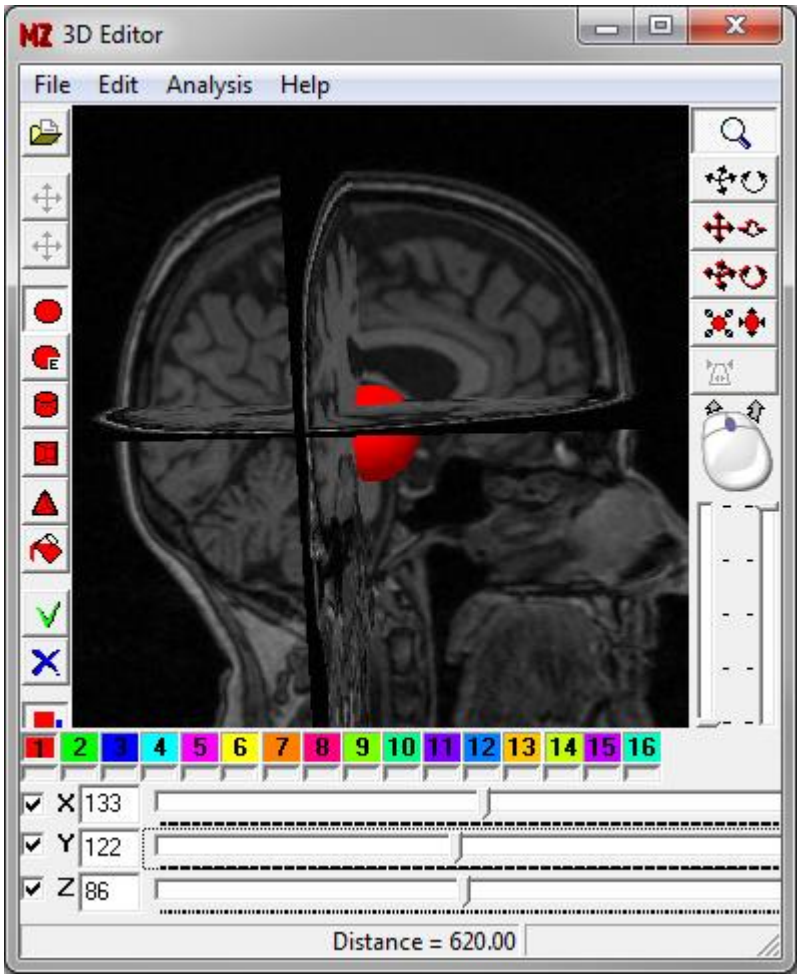

Figure 2.4. *Screenshot of MaZda (version 4.6) 3D Editor window.*

The MaZda software, being discontinued since 2006, does contain some shortages and the latest methodologies from recent research can no longer be experimented using MaZda to its full potential. This thesis is aimed to revise some of these shortages by implementing a frame for a completely new application for texture analysis of MRI. Detailed review on MaZda and its features is presented in Chapter 3.1.

2.4 Texture analysis at TAUH

The MICHP of TAUH provides a direct contact for the researchers to the hospital personnel and access to the imaging equipment if necessary. This allows fluent interaction and a valuable link between the technologically oriented professionals and the multitude of healthcare experts. Supervised by Professor Eskola and MD Dastidar the research group had produced extensive research on texture analysis using MaZda for several years with various MRI modalities and for multiple different diagnostic cases.

2.4.1 Non-Hodgkin's lymphoma

MRI can be effectively used to distinguish between different soft tissue types as described in Chapter 2.1. This includes identification of lymphomas. Harrison *et al.* [46;

47] researched the possibility of using texture analysis in classification of non-Hodgkin's lymphoma (NHL). Treating cancer patients over long periods of time with chemotherapy is used for containing or removing the malignant tissue altogether. The follow-up was performed by taking three consecutive MR images of the patients' abdomen. From three to five slices were selected as image series for analysis. Using MaZda for texture analysis of patients during the therapy period proved promising results and the chemotherapy response was successfully classified using T_2-images of the diagnostic stage and second evaluation stage. The inhomogeneity between slice thicknesses of the images, manual ROI selection and ROI size were considered as the probable cause of error in the discrimination process. The research was conducted under Tumour Response Evaluation (TRE). [46; 47]

2.4.2 Multiple sclerosis

The imaging arrangements have great value on the result of the texture analysis process. Savio *et al.* [48] have researched the process of determining the sufficient slice thickness for MRI of multiple sclerosis (MS) lesions. Sequence selection compatible to the analysis type, highest possible magnetic field strength, minimum voxel size, patient stability during imaging, noise and slice thickness all influence the image acquisition process and ultimately the output image data. With intensity averaging three sequential 1-mm slices were combined to create a simulated 3-mm slice using MATLAB. For both original and simulated images a white matter, an MS plaque adjacent white matter and an MS plaque located ROIs were drawn in MaZda. After performing both linear and non-linear discretion analysis it was determined that the simulated 3-mm slice was indeed sufficient in performing reliable classification of MS lesions. To compromise between thin slices to reduce SNR and thick slices to keep the texture data was proven essential. [48; 49]

2.4.3 Femoral neck

With proper sequence selection MRI can be effectively utilized in analysis of hard tissues. Fast Low Angle Shot (FLASH) and T_{2*} multi echo data image combination (MEDIC) sequences were applied by Harrison *et al.* [49] to detect differences of trabelucar or cancellous bone of the femoral neck. Hip fracture is often regarded as age-related but the research focused on effects caused by long-term loading *i.e.* exercising. Respective to their activity type the female athletes of top national level were divided into high-impact, odd-impact, high-magnitude, low-impact and non-impact groups. The referral group contained healthy non-athletes. Three co-occurrence matrix parameters were calculated for both image sequences using MaZda. Weak spatial resolution of 0.9 mm produced by the 1.5T scanner could not distinguish the single 0.1-mm thick trabeculae thus forcing the research to rely on estimates. In addition, a challenging setting of six groups and four regions of interest on the trabecular bone required manual

analysis and fully automated procedures were called for especially for larger groups of image data. [49]

2.4.4 Mild traumatic brain injury

Holli *et al.* [50] have researched the changes in cerebral tissue of the brain caused by mild traumatic brain injury (MTBI). MTBI is considered the most common type of brain injury, but many imaging modalities are struggling to provide visually distinct data of such subtle changes. To test the efficacy of texture analysis on finding this divergence patients were imaged with MRI within three weeks of the trauma and ROIs were selected on the segments of the brain that have been found sensitive to damage. Using MaZda ten most prominent texture features were chosen for final analysis. Co-occurrence matrix, run-length matrix and wavelet-based parameters were resulted in significant statistical differences in corpus callosum segment. Without in-depth knowledge of the origin trauma, placing the ROIs was challenging and may cause pertinent damaged tissue to be unnoticed. [50]

In further research DTI was used and texture analysis was applied to the same ROIs with the patients undergoing a series of neurocognitive tests. A correlation between memory tests and texture parameters was discovered thus suggesting that the combination of texture analysis and DTI may be used in MTBI diagnosis. [51]

2.4.5 Breast cancer

Mammography and ultrasound are the most traditional modalities related to breast cancer diagnosis but breast MRI (BMRI) has also emerged as a feasible alternative for diagnosing and detection. Among twenty patients with both lobular and ductal types of either primary or recurrent breast cancer a classification accuracy between 80% and 100% was achieved co-occurrence matrix providing the most suitable discrimination parameters. [52]

2.4.6 Parkinson's disease

Detecting anomalies in the brain tissue as early as possible provides increased chances of successful diagnosis and treatment. In Parkinson’s disease (PD) the structural changes in the brain MRI are very subtle and texture analysis has been applied to both diagnosis and follow-up of the patients. Textural analysis was successful in discriminating the differences with the selected co-occurrence matrix-based parameters in thalamus and corona radiata in a longitudinal study. In the interhemispheric comparison differences were most significant in basilar pons and midbrain. In addition to this, a relation between clinical characteristics and the texture parameter was found in both cases. [53; 54]

2.5 Texture analysis abroad

Despite the fact that MaZda is no longer under active development it is actively capitalized worldwide. Focus of these studies is clearly in brain MRI providing possibly the most challenging environment for medical image analysis for both visual and computational methods alike.

2.5.1 Alzheimer's disease

Alzheimer's disease (AD) has been one the most intensively researched disorders in recent years. Similarly to all degenerative disorders progressing in the brain, the damage is often irreversible and increases exponentially with time urging the early-stage detection procedures to be accurate and reliable. Dementia on elderly is known to be caused by AD which symptoms range from memory loss and disorientation to complete lack of communication skills and the inability for the patients to survive on their own. The diagnostic accuracy of the traditional non-computerized method was found to depend highly on the geographic location and varies between 75% and 90% in developing countries and developed countries respectively. [55]

In order to improve the accuracy further texture analysis was introduced for AD diagnosis. Patients with moderately severe or severe dementia were included in order to receive higher discrimination results. With the 3D texture features of co-occurrence matrix in the hippocampus higher spatial resolution and improved sensitivity compared to 2D techniques was anticipated. Using MaZda over 100 texture features were extracted from the three 3D ROIs placed in the hippocampus and entorhinal cortex decreasing in volume. The classification was performed with all the image data as training set and using the significant feature and Fisher approach the former resulting in rather low accuracy of 64.3% and the latter resulting in high accuracy of 96.4% regardless of ROI placement. Correlation between texture analysis and the results from the screening procedure conducted for the patients involving mini-mental state examination (MMSE) was also found. [55]

2.5.2 Juvenile myoclonic epilepsy

Epileptic patients are susceptible to seizures and loss of control of their motoric functions which may lead to serious hazards if encountered unattended. The juvenile myoclonic epilepsy (JME) is normally diagnosed using electroencephalogram (EEG) but minor abnormalities may be detected by visual analysis [56]. However, the accuracy of detecting epilectogenic lesions based on MRI reached only 50-60% with 1.5T field strength [57]. The cause of epilepsy remains unknown but the origin has been pinpointed to the thalamus. By applying MaZda texture analysis methods differences between texture parameters were shown when comparing visually undetected JME patients and the control group. [56]

2.5.3 Parotid gland lesion

Surgical planning is common to benefit from 3D MR images especially in high risk brain areas. Benign and malignant mass discrimination in parotid gland has been reported inconclusive even with distinct contours and high quality image data. High-grade lesions are also reported with low intensity and inaccurate contours on both T_1- and T_2-weighted images that are rarely detected by visual analysis only. Since the diffusion of water is decreased in malignant tissue such as lesions DWI was utilized for optimal intensities and apparent diffusion coefficient (ADC) values. Patients with parotid gland lesions who underwent either surgery or biopsy were imaged prior to and after the procedures. Both manual and automated segmentation was applied using MaZda for ROI delineation process. OsiriX software was used for DWI analysis of ADC values and the statistical analysis was carried out with Statistical Package for the Social Sciences (SPSS). By using texture analysis the retrospective study succeeded in discriminating not only Warthin tumour and pleomorphic adenomas but also differentiating between benign and malignant masses which could not be achieved with the DWI ADC value analysis. [58]

2.5.4 Posterior fossa tumour

Paediatric brain tumours in posterior cranial fossa region are reported to cover 20% of the brain tumours of children [59]. Despite the promising results from quantitative image analysis observed in DWI the routinely acquired T_1- and T_2-weighted MR images are rarely utilized in further analysis. Conventional MR images of paediatric patients with pilocytic astrocytomas, medulloblastomas and ependymomas of posterior fossa were used in MaZda for texture analysis. The ROI selection was completed by manual delineation in ImageJ from where the data was imported to MaZda. Further principal component analysis (PCA) applied in commercial Minitab 15 software for statistical analysis. Another commercial tool called DTREG was used for classification based on the local discriminant analysis (LDA) of MaZda. [60]

2.6 Software development in medical informatics

The healthcare sector covers a great number of individual organizations and units that are devoted to dealing with extremely elaborate problems ranging from worldwide epidemics to the nanoscale. Medical image processing can be regarded as part of this entity but also belonging to medical informatics in a sense that the image acquisition systems produce data that is further processed by computational methods. Standards in medical informatics are required for unambiguous communication, secure digital data transfer between systems as well as diagnosis and procedure codes. An example of such standard is the use of same coding schemes in sending clinical data to a central database. Without agreements upon common terminology all communication would be impossible. Timing is essential in developing common practises for medical

informatics. If the proposed standard is deemed unnecessary it may be disregarded altogether. Introducing a standard too late may result in similar reaction due to the hardened routines of people. [61]

Considerable amount of resources has been targeted to the data-interchange standards in medical informatics. The communication between the sender and the receiver requires the content and format being sent to be standardized. The open systems interconnection (OSI) model has been implemented for this purpose. For a successful communications transaction seven levels of specification is to be fulfilled: physical, data link, network, transportation, session, presentation, and application level. The application level defines the data content of the transaction message according to a specific vocabulary or semantics. Unfortunately there are several code sets used for determining the data group content of the transaction message which ultimately is completely against the purpose of the data-interchange standard. Most of the medical data is generated by imaging systems and without ensuring a standardized and fluent data transfer process throughout the healthcare system the adverse effects can be carried on even to the image analysis process. [61]

The field of medical informatics or medical image processing is rarely regarded as a typical software development environment. Open-source solutions are common for many reasons. The research-oriented context prefers sharing information to creating economical profit. Without the profit responsibility and financial pressure of the industrial approach there are less expectations towards the end product in non-commercial projects. With the information technology skills broadly applied across all scientific fields the developer of the application can often be the same group conducting the research. Unlike in the conventional software development business there exists no dedicated standard in medical informatics for conceptual small-scale software development practises to support the process.

The concept of creating specific light-weight guideline for software development in medical informatics was inspired by a project called CERES. The CERES project was carried out at the Department for Medical Informatics of Aachen University by a team with versatile backgrounds from many different branches of science. Based on this instructive experiences with the project a set of guidelines in medical informatics research projects were introduced. The proposed guidelines are generated in six individual steps that form a cyclic process. The first step is the careful identification of the problem, the needs and solutions. In the following steps from two to four a guideline is proposed and reviewed before a final revision is made. The guideline is authorized in step five and step six involves periodic reviewing and updating. [62]

The IEEE 610.12-1990 Standard Glossary of Software Engineering Terminology sets the following qualities for software: correctness, reliability, efficiency, integrity, usability, maintainability, flexibility, portability, testability, reusability and interoperability [63]. Another example of industry-level process model is the ISO/IEC 25010 standard for Systems and software Quality Requirements and Evaluation

(SQuaRE) [64]. For a minor software development project such requirements and criteria are a challenge but even loosely following these guidelines can improve the quality and understandability of the source code significantly. [62]

3 METHODS AND MATERIALS

The implementation process was started with requirements analysis presented in Chapter 3.3. This process involved meetings with the research group members and close interaction at the TAUH premises on a daily basis. The group had been experimenting with MaZda for several years and based on their experience and input the original software application design was sketched.

From the results of the studies described in Chapters 2.4 and 2.5 additional perspective was discovered to support the software design process. The MaZda software features are introduced in Chapter 3.1 and MATLAB environment and the key components involved in this theses are reviewed in Chapter 3.2 respectively.

3.1 MaZda package features

MaZda (version 4.6) is a standalone software compatible with Windows® XP operating systems onwards and it contains separate tools for 2D and 3D textural analysis. The software supports macros that can be created for running automated commands regarding the analysis process including all the adjustments available manually in the GUI. MaZda can also be extended with plugins by creating a macro with a ".plugin" file extension.

3.1.1 Texture analysis flow in MaZda

The typical texture analysis flow in MaZda is depicted in Figure 3.1. The flow starts with the standard procedure of loading the existing image data to more suitable format for the program to process. MaZda supports digital imaging and communications in medicine (DICOM), Windows Bitmap and raw file format images of either 8 or 16 bits. The next step is ROI selection. Up to 16 regions or groups of regions can be drawn using either spherical, elliptical, rectangular or polygonal tools. After drawing the ROI it can be freely relocated, duplicated, saved or loaded from disk. The third step involves texture feature estimation which calculates up to 275 parameters for each ROI present. Option of pre-estimation image normalisation is provided reducing the variance between the texture parameters. The texture features consist of 9 histogram-based, 11 co-occurrence matrix-based in four directions and with five distances, 5 run-length matrix-based, 5 autoregressive model-based and 16 Haar wavelet-based parameters. These parameters are presented in report format. Data aggregation and feature selection can then be applied to find a more compact subset of parameters. The criteria available for feature selection are Fisher criterion and the minimization of classification error and

correlation coefficient (POE+ACC) criterion. Both methods select ten most prominent features from the given set. Alternatively feature selection can be done also manually. This concludes the MaZda texture analysis flow and the selected parameters can be passed to b11 module for further processing. [5; 44]

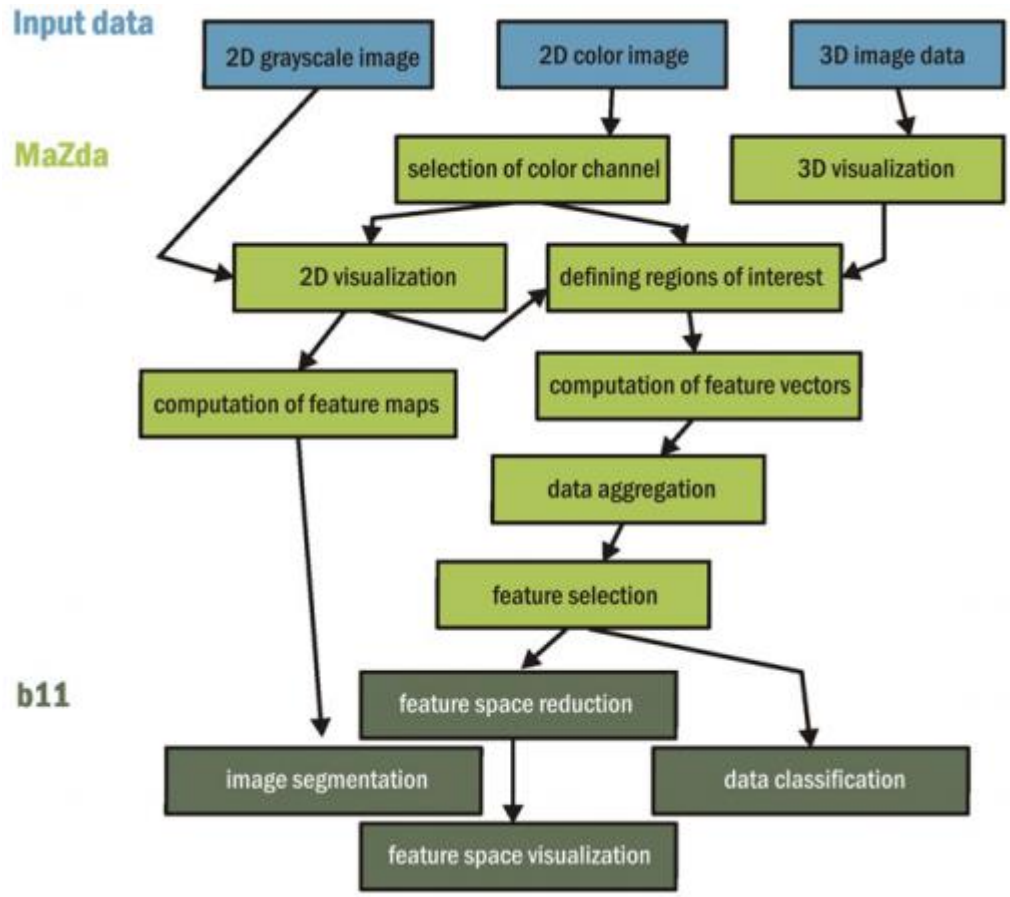

Figure 3.1. *Mazda and b11 combined texture analysis flow. [43]*

3.1.2 b11 component

The b11 software provides additional functionality to support and complement the texture feature analysis flow started in MaZda. The component is installed with the MaZda package and it can be run directly from MaZda report window after feature selection process or completely independently. The b11 module consists of feature space reduction and visualization, image segmentation and data classification. In feature space reduction the original features are narrowed down by applying either PCA, LDA or nonlinear discriminant analysis (NDA) to create a projection of the extracted features. The image segmentation in b11 is based on feature maps calculated by unsupervised method of k-means clustering. The feature vector classification is aimed for examining the ranking between the feature vector values. For the classification process b11 supports nearest neighbour (1-NN) and artificial neural network (ANN) classifiers for both raw and processed data. The b11 module is also capable of

visualizing the feature vectors that have been analysed after applying feature space reduction. [5; 44]

3.2 MATLAB programming environment

Developed by MathWorks and originally released in 1984 the MATLAB environment is an interpreted high-level multi-purpose programming platform. MATLAB is a popular tool in academic research and education but less widespread among the general public due to licence fees. MATLAB is based on just-in-time (JIT) compilation common to many interpreted languages. JIT compilation is dynamic translation of code into machine language during the program execution. This run-time execution differs from conventional compilers that require execution before the application is run. [65]

MATLAB has characteristic notation or language called M-code that resembles other traditional object-oriented programming languages like C++ and Java. Declaring variable type and size differs from other languages due to JIT compilation enforced by the platform thus the language is considered weakly typed. This means that the type and size of each variable can be left undetermined and run-time compiler will conclude appropriate values to be selected. This allows a generic approach for projects of low complexity but does not match with more computationally demanding tasks. One of the defining characteristics of the language is that all data types are arrays or matrices. This enables excellent mathematical properties. All variables in MATLAB are stored to and loaded from the workspace. The visibility of these variables varies but in general there are two types of variables with either local or global visibility. Local variables being accessed only by the executing block the global variables can be accessed more freely. This link is achieved by handles which can be regarded analogous to pointers in other languages. [65]

Despite the fact that performance is very system-dependent, optimization of the programming language reduces loading times and enables more fluent flow for the user. With most of the programming languages this can be tracked down to memory optimization. In MATLAB there are several ways to improve the performance of the implementation. Storing and accessing data in columns, pre-allocating memory before accessing it and avoiding unnecessary variable creation can be effective methods in enhancing the computational performance of the software. [65]

MATLAB offers a possibility to take advantage of code created in C, C++ or Fortran languages. This requires compiling the code into a MATLAB Executable (MEX) file. A dedicated function named as *mexFunction* needs then to be included in the *main* function of the application that is being linked to MATLAB. Via the *mexFunction* data can be transferred between the two languages. In addition to MATLAB only a supported C or Fortran compiler is required. Likewise MATLAB code can be accessed from the C or Fortran standalone programs via pipes in UNIX or through ActiveX on Windows®. In addition M-code can be converted into a shared library in C or C++ using MATLAB Compiler. [65]

3.2.1 Image Processing Toolbox

Image Processing Toolbox (IPT) is a complimentary library package extending MATLAB and focusing on image processing, analysis, visualization and algorithm development. IPT provides a range of functions for image analysis, enhancement, registration, segmentation, morphology, transformations and statistics. All the functions are general-purpose building blocks that can be efficiently used in supporting the implementation of any MATLAB application.

Four types of images are supported by the IPT: indexed images, intensity or grey-scale images, binary images and RGB images. In addition to image reading, writing and displaying (loading to workspace, saving hard disk and visualising in figures respectively) IPT features also more scientific and even medical image processing specific functions such as DICOM-related methods.

For 2D ROI managing purposes IPT contains both drawing and editing functions. Selection, filtering and filling of the ROI from an image can be performed by applying a binary mask matrix. Polygonal, rectangular and elliptical drawing tools are available for creating the mask. Delineating the ROI is performed by clicking or dragging the mouse over the area of interest.

For the texture analysis features the most helpful attribute is the grey-level co-occurrence matrix (GLCM) function *graycomatrix*. The *graycomatrix* function input parameters consists of the 2D image data matrix *I*, a gray-level scaling vector identified as *'GrayLimits'*, an integer determining the number of gray-levels used for scaling indentified as *'NumLevels'*, an array of offsets describing the angle identified as *'Offset'* and a Boolean value that determines if symmetry is allowed identified as *'Symmetric'*. Default values are set for unscaled, eight grey-levels with a 0° angle and asymmetric calculation. The resulting matrix *p(i,j)* that can be passed as input to the GLCM properties function *graycoprops* accompanied with the property name *'Contrast'* (3.1), *'Correlation'* (3.2), *'Energy'* (3.3) or *'Homogeneity'* (3.4) respectively. [66]

$$\sum_{i,j} |i-j|^2 p(i,j) \tag{3.1}$$

$$\sum_{i,j} \frac{(i-\mu_i)(j-\mu_j)p(i,j)}{\sigma_i \sigma_j} \tag{3.2}$$

$$\sum_{i,j} p(i,j)^2 \tag{3.3}$$

$$\sum_{i,j} \frac{p(i,j)}{1+\ |i-j|^2} \tag{3.4}$$

The expected values μ_i and μ_j and standard deviations σ_i and σ_j are used for calculating the correlation of GLCM in (3.2).

3.2.2 Graphical User Interface Layout Editor

For the layout design a Graphical User Interface Layout Editor (GUIDE) was used. This toolbox is embedded in MATLAB and provides a GUI for creating GUI. GUIDE can be operated by both interactively and programmatically or programmatically only. This means that a GUI created using GUIDE can be modified in M-code format but creating a GUI programmatically in M-code blocks the option of using GUIDE later on in that particular project. With the interactive option a GUI editor is opened. Each GUI element or window created using the editor is saved as MATLAB figure (.fig) file. The GUI provides all the available elements including the buttons, panels, text fields and tables etc. that can be created and edited accordingly. The element properties can be accessed via Property Inspector view that contain the detailed specifics of that particular element. All elements are identified based on tags. Each figure file has a corresponding M-code file that is created automatically and updated every time the figure file is modified through using either the GUI editor or the standard M-code text editor. Dedicated editors for menu editing (Menu Editor) and toolbar editing (Toolbar Editor) can be accessed via GUIDE menus. GUIs are operated by functions called *callbacks* which "call back" MATLAB for any given purpose. These *callbacks* are triggered by the end user via interacting with the GUI and creating an event in the process. In GUIDE the developer's task is to assign these events to appropriate *callbacks* according to the desired purpose.

3.3 Requirements analysis

Main focus in creating the software frame with MATLAB was on future extensions, usability and compact features. No readily available basis were used in implementation of the software but only the native built-in toolboxes provided in MATLAB (version 8.1.0.604 R2013a) as described previously in Chapters 3.2.1 and 3.2.2. The design and implementation process was mainly left without strict requirements or limitations which allowed great possibilities for experimenting with different approaches and solutions. Naturally some principal guidelines were introduced.

MaZda (version 4.6) software was regarded as the reference and source of comparison in case of any need for debriefing or consultation. In terms of the software data structures and GUI design no specific requirements were set since the software would be used only in within the MATLAB platform and no explicit expectations existed among the research group members. Data visualisation and ROI selection were considered the most time consuming phases of this project and special emphasis was introduced to these entities in early design process. For the initial version only rectangular cuboid ROI drawing style was required with the ellipsoid style being second in priority. Regarding the texture feature parameter functionality implementations the

requirement was referenced as an unknown variable since estimating the total workload proved to be challenging. 3D GLCM and LBP were the two most desired features in addition to the basic histogram-based feature parameters.

4 RESULTS

The software design process was started with the selection of programming language or platform that would be used for the implementation. This was done based on the decision that a completely new application would be implemented instead of extending an existing one. Even though the actual programming platform options were not limited in the software requirements only two programming languages were ultimately considered. With most people involved in the process having previous experience working with C++ and MATLAB platforms the ruling out of other available options came naturally. C++ was regarded for its object oriented and generic properties with excellent performance but high complexity. MATLAB on the other hand would offer a wide range of built-in features for visualization and mathematical modelling such as IPT as well as user interface design such as GUIDE in a commercial environment. In addition MATLAB's support for other programming languages via a special interface such as Java, C and C++ was regarded as a benefit.

With the comprehensive tools for image and signal processing accompanied with high-level script-based programming language MATLAB was selected as the platform for implementing the software. The objective of the requirements analysis and design was to take advantage of solutions that would allow features to be readily added later on. This extensibility was met with MATLAB and it provides a more agile approach to anyone interested in further developing the image processing tool in the future. To avoid any possible cross-platform difficulties the implementation process was carried out on Windows® 7 Professional (Service Pack 1) operating system, which was also used by the texture analysis research group. For the test data brain MR images acquired using Siemens 1.5T in DICOM format were used.

4.1 Data structures

For efficient processing of image data in MATLAB workspace data structures for *Study*, *ImageSeries* and *ROI* were introduced with filename extensions ".sty", ".is" and ".roi" respectively. Utilizing object oriented approach to classify these core components the hierarchy of the software application was consciously made compact and linear. The process of storing the application data during the work flow would be facilitated easily with these encapsulated integrities already available.

The main data structure and highest class in the hierarchy is called *Study* which represents the entity of the image processing project withholding handles of both Study manager module described in 4.2.2 and Visualization module described in 4.2.3. The *Study* also aggregates all *ImageSeries* structures that are stored in a list. These instances

consists of the information regarding the three dimensional image stack matrix created from the images loaded by the user. The *ImageSeries* data aggregates all *ROI* structures stored in a list. The *ROI* instances hold only distinctive information regarding a single ROI *i.e.* the spatial coordinates and appearances. The class diagram of the core components is shown in Figure 4.1.

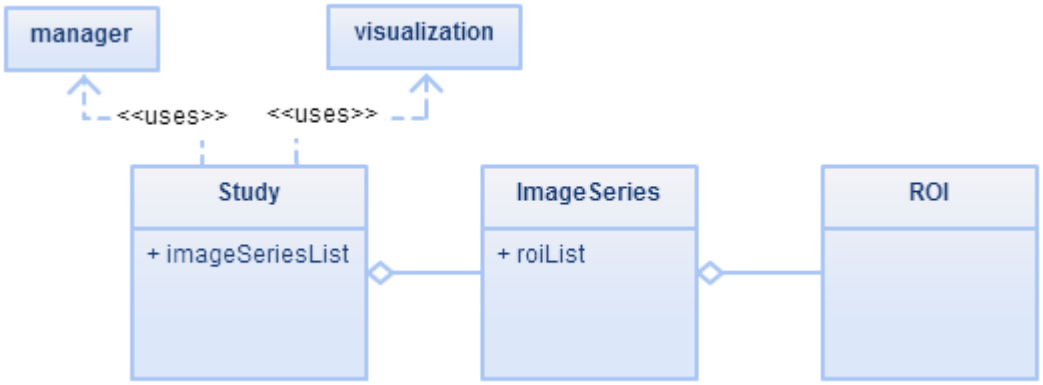

Figure 4.1. *Class diagram showing aggregation between Study, ImageSeries and ROI.*

Similar structure was implemented for the folder hierarchy that would contain all information saved using the application. Illustration of this hierarchy in traditional folder-file format is demonstrated in Figure 4.2.

Figure 4.2. *Folder hierarchy after saving exampleStudy file with imageSeries1 folder including ROI1 and ROI2 and imageSeries2 folder including ROI3.*

Selected features are saved to the root folder of the Study in progress. File formats supported for saving the feature parameters are Microsoft® Excel® spreadsheet (.xlsx) and MATLAB MAT-file (.mat).

4.2 Software modules

The software frame was designed to consist of three detached modules (*i.e.* windows) which the user can operate individually. This allows the user to have full control on how to position the modules on screen or over multiple screens. The complete layout design is presented in Appendix 1. The function of each module is described next with screenshot images attached to demonstrate the GUI.

4.2.1 ImageAnalyzer

The main module, called the ImageAnalyzer, consists of a menu bar only as shown in Figure 4.3. This module controls one Study manager module at a time by creating new *Study* instance, loading already saved *Study* or saving current *Study* via the File menu. The Feature Extraction menu, discussed in more detail in Chapter 4.3, allows the user to select the desired features by checkbox selection. Feature sets can also be saved and loaded for more convenient use in other *Studies*. The Classification menu and Result Evaluation menu are examples of the extensibility that this module holds for future development.

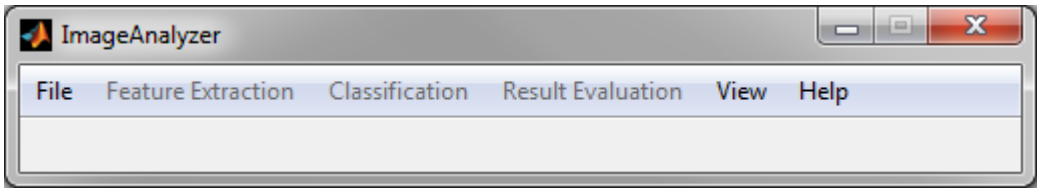

Figure 4.3. *Screenshot of ImageAnalyzer main menu module.*

For more convenient visual presentation the content of each main menu item can be observed from the MATLAB Menu Editor view depicted in Figure 4.4. Adding new algorithms or features can also be done by creating a new menu item using the GUIDE Menu Editor. Each software module can be configured either editing the MATLAB figure file or the corresponding M-code file.

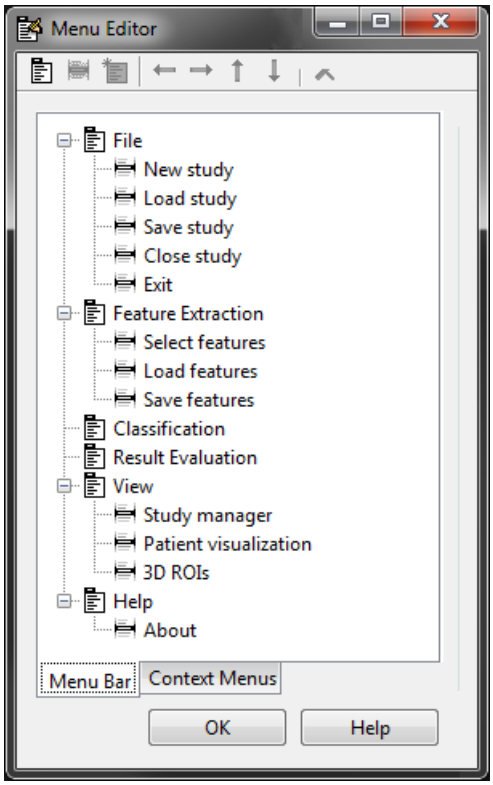

Figure 4.4. *Screenshot of Menu module viewed in GUIDE Menu Editor.*

4.2.2 Study manager

Named after the data structure in Chapter 4.1 the Study manager module functions as the medium for handling *ImageSeries* data. The main function of the module is to provide means to load the image data in to the MATLAB workspace variables. The Study manager also controls the Visualization module introduced in 4.2.3 and offers the functionality to name and delete *ImageSeries* instances. The module displays the user information about the image set that is currently being processed including number of slices, image resolution and ROI details as shown in Figure 4.5. Additional editable elements present in the module are the physical dimensions of the digital data. The information regarding the pixel values are not present in the metadata of other than DICOM format images. Supporting other image formats was valued early on the process thus presenting these elements was required. By changing the physical pixel dimension values the mapping can be visually verified by the user on the Visualization module instantly so that the chance of misinterpretation would diminish.

Reducing the number of times the images are loaded to minimum was essential in keeping the work flow as fluent as possible. Switching between *ImageSeries* sets is done by selecting the saved *ImageSeries* from the dropdown menu removing the need for a complete reloading of the application. Several dozens of sets of images can be stored into a single *Study* limitation being the size of the display and how many dropdown menu items can be shown at once.

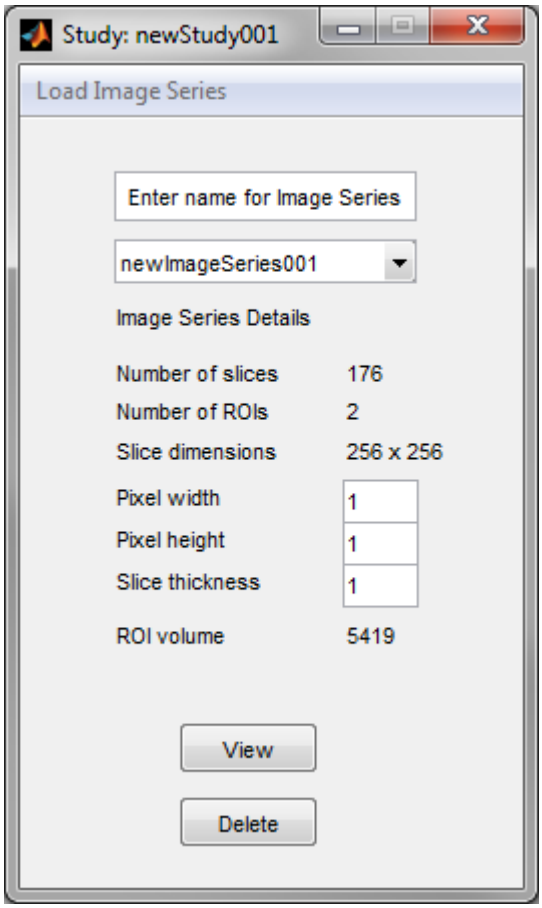

Figure 4.5. *Screenshot of ImageAnalyzer study module.*

4.2.3 Visualization

After loading a set of images using the Study manager module the user is presented with the Visualization module shown in Figure 4.6. One *Study* saved in to the Study manager at a time will be presented in the Visualization module. The module displays the sagittal, transverse and coronal planes of the 3D matrix comprised of the 2D image data. Each projection is using the same image stack data from a 3D matrix by only shifting the angle of view. Each planar view can be scrolled by using the slider tool which also displays the slice number of the image on that projection. The original imaging plane is shown with the original image resolution and the other visual resolutions are based on the number of slices loaded.

The ROI/VOI handling features are located on the bottom part of the module. Determining regions of interest was recognized as the most time consuming phase of the image analysis flow hence simplicity was emphasized while designing the GUI. Drawing a ROI is started with the shape selection. The creation of rectangular regions of interest was implemented with *imrect* function available on MATLAB. This function allows coordinates to be saved on any of the three 2D planes by creating a rectangular cuboid which would work as a mask to the image data matrix containing the selected volume data. By inserting the ROI in the sagittal view the corresponding views are automatically scrolled to the slice that has the ROI displayed. Initially the ROI is 2D

and only a line of one pixel in width is visualized on transverse and coronal views. By extending this line the ROI can be given volume thus completing the transformation from 2D to 3D and ROI to VOI. In order to distinguish ROIs from one another they can be individually named and coloured. The colour and transparency can be adjusted by the R (red), G (green), B (blue) and Alpha sliders accordingly. The ROI visibility can also be set via checkbox selection either individually or applying the change to all ROIs.

The ROI data structure introduced in 4.1 allows ROIs to be handled completely separately to the *Study* and *ImageSeries* files. Saving any ROI will create a new file which can be imported to any other image set in any other *Study*. Multiplying an existing ROI with the copy feature will add a replica of the currently active ROI to the *ImageSeries*. The name of the new ROI will be automatically edited to contain a suffix. Loading a previously loaded ROI will add a new ROI to current *ImageSeries* renaming the file with a suffix if necessary.

Figure 4.6. *Screenshot of ImageAnalyzer visualization module.*

By clicking the 3D button a 3D visualization window will pop up. This currently supports only a coarse view with the ROI data.

4.3 Feature selection

The feature selection window shown in Figure 4.7 can be accessed from the Menu module. The view describes all the texture feature parameters available for the user to choose from by simple checkbox selection. By default all the features are selected. Histogram-based features of standard deviation, mean, variance, skewness and kurtosis are supported and readily available in MATLAB IPT.

The MATLAB implementation of LBP (version 0.3.3) is readily available on the Department of Computer Science and Engineering at the University of Oulu webpage

[67] based on the publications of Ojala, Pietikäinen and Mäenpää [25; 26]. The *lbp* function input parameters consist of the image matrix *I*, number of sampling points *N*, radius *R*, mapping type and mode. The mapping type options are *'u2'* for uniform LBP, *'ri'* for rotation-invariant LBP and *'riu2'* for uniform rotation-invariant LBP accordingly. A separate *getmapping* function is called to create a table fitting the desired LBP type. The mode value options are *'h'* and *'hist'* for histogram of LBP values and *'nh'* for a normalized histogram respectively. Default values are set for eight sampling points with a radius of one, no mapping and a non-normalized histogram.

The co-occurrence matrix-based features for 2D analysis are calculated using the *graycomatrix* and *graycoprops* included in IPT and described in Chapter 3.2.1. For 3D GLCM an implementation of *cooc3d* function created at the DePaul University College of Computing and Digital Media in Chicago was embedded [68]. In addition to a 3D GLCM a Haralick feature vector is calculated as the *cooc3d* function output. The Haralick vector features include energy, entropy, correlation, contrast, variance, sum mean, inertia, cluster shade, cluster tendency, homogeneity, maximum probability and inverse variance. Input parameters for the function consist of a 4D image matrix, the number of grey-levels, an array of distances and an array of direction offsets. The image matrix is 4D containing a number of 3D image data sets so that all 3D image sets, such as multiple ROIs, can be calculated at once. The number of grey levels can be set if rescaling the intensity values is required. The distance array determines the length used for calculating the co-occurrence matrix and the directions array determines the angle from which the calculation is propagated. In addition to the four directions of 2D GLCM (0°, 45°, 90°, 135°) nine 3D space dedicated directions are available. Default values for the array for distances is [1, 2, 4, 8] and for the default directions all available 13 angles are selected.

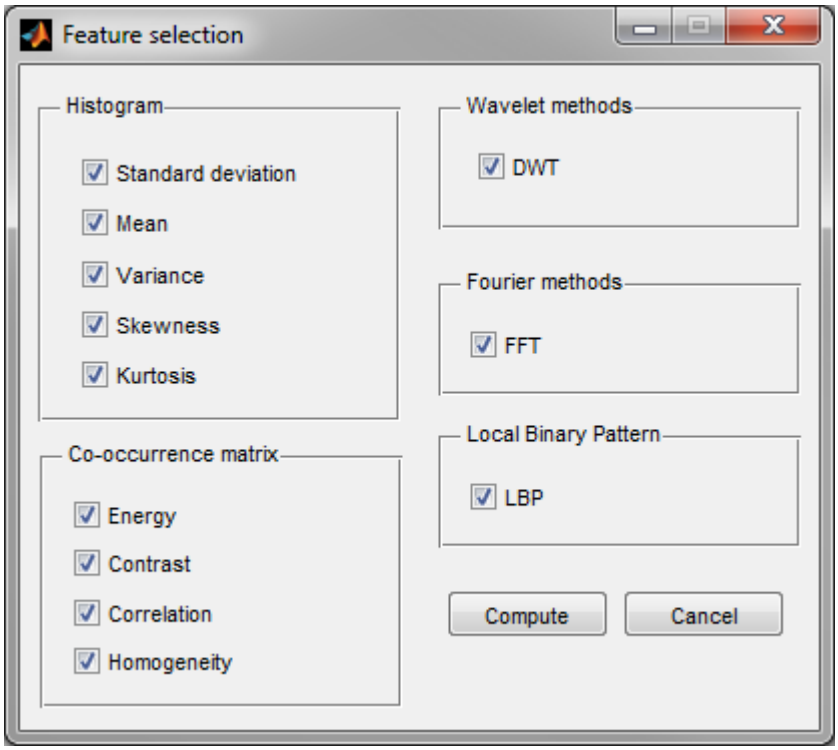

Figure 4.7. *Screenshot of ImageAnalyzer feature selection window.*

Clicking the compute button begins the selected calculations for all the *ROIs* saved for the active *ImageSeries* of the *Study*. The results are saved in a single .xls file format to the folder containing the *Study*. For each *ImageSeries* a new sheet is created to contain the data. The parameter values are listed by columns and the rows represent the *ROIs* as shown in Figure 4.8. The user is prompted with a dialog asking if the created file should be opened directly.

	A	B	C	D	E	F	G	H
1	ROIName	STD	Mean	Variance	Skewness	Kurtosis	Energy	Contrast
2	ROI1	180,9932	305,7981	32758,52	1,097883	2,581557	0,08375	0,575163
3	ROI2	177,2974	378,7279	31434,37	-0,17225	3,135643	0,063712	0,848297

newImageSeries001 newImageSeries002

Figure 4.8. *Screenshot of ImageAnalyzer feature parameters exported to Excel®.*

4.4 Distribution

For distribution and maintenance purposes a GitHub repository was created for the *ImageAnalyzer* project (varjojukka/ImageAnalyzer). GitHub provides a web-based service for version control of software development projects. With the integrated social networking features an interactive platform for example improvement requests and update change logs is readily available for everyone to access and contribute. The *ImageAnalyzer* code was also made available in MATLAB File Exhange web-page that hosts a free community to sharing scripts and applications created with MATLAB.

5 DISCUSSION

Variation between different open-source medical imaging software tools and lack of multipurpose application relates to the underlying feature of healthcare systems – the vast diversity. Repeatability and data collection remain unresolved issues in MRI that also have an effect on texture analysis. Clinical systems continue to focus on dedicated solutions but the pressure on medical information systems to provide data that can be accessed for other than the original primary purpose is expected to reflect on medical image processing also. However, problems related to computational limits caused by the multidimensional structure of data are expected to diminish with the technological achievements becoming increasingly common and more affordable. Experts of information technology and engineering collaborating with the medical doctors, radiologists and other healthcare personnel is vital in achieving the most comprehensive CAD solutions for clinical environment.

Based on the analysis of open-source medical image processing software no competition to MaZda was found for texture analysis of MR images. Thus results performed by different software than MaZda was not available for comparison. It was also noted that some studies failed to report the reference for the software tool involved in the texture analysis process. Undocumented custom implementations for texture analysis purposes may hereby exist.

5.1 Platform analysis

The benefits and drawbacks in using a platform dependent commercial software for the foundation of medical image processing frame with potentially wide range of contributors and end users were analysed in collaboration with the texture analysis research group prior to implementation. Even though MATLAB has prominent presence in the academic world as a versatile educational and research tool, the commercial software background may cause unwanted dependencies. Changes in the commercial licensing agreements and version updates of MATLAB may directly or indirectly affect the *ImageAnalyzer* software thus monitoring the development of the platform is required. This can be achieved for example by following the MATLAB Central community as a registered user. The need for updating the software to match MATLAB version has to be taken into consideration every iteration preferably with minimal delay between the platform update and *ImageAnalyzer* modification. The implemented software or some of its added content may suffer from these updates. These may include changes in MATLAB interface or functions causing compiling or run-time errors.

However, major reformation is not expected since recently MathWorks has released one or two updates per year for the platform.

From the group of image processing software introduced in Chapter 2.3 three still are or originally were developed in C++. This majority is partially explained by the early origins of the applications when options were more limited. A trend towards Java-based imaging software is indicated by the evolution of personal consumer devices. This was recognized especially among the applications with "extendibility by plugins" approach. The fundamental principle of Java is the platform-independent architecture that still is regarded as a great asset. The era of portable and tablet devices may be at hand but for medical image processing industry they hardly provide solutions.

5.2 GUI

Even though medical image processing software differentiate from other image processing software mainly based on diagnostic and statistical features, the GUI design cannot be disregarded. Compromising between usability and functionality is a delicate process and several approaches to this problem were observed while analysing the open-source image processing software in Chapter 2.3. The image data should be easily accessible, most important parameters constantly visible and preferably the GUI would be configurable according to the end user preferences. 3D image data coupled with hundreds of parameters rises a challenge for GUI design to find optimal solutions for providing access to or visualizing this vast amount of information compactly and discernible at the same time. While MaZda and 3DSlicer represent the one main window approach with toolbars and menus attach to the sides, a completely opposite approach is used in ImageJ with a bare menu bar confining all the functionality in the submenus, hidden from the view.

Drawing the ROI manually is still the standard option in quantitative texture analysis even though sophisticated automated segmentation applications are available such as the ITK library. This was confirmed in all of the studies presented in Chapters 2.4 and 2.5 respectively. It was also concluded that the ROI drawing process requires time and a skilled medical professional to succeed. Manual delineation on 2D was observed superior to 3D. Extensive ROI editing options will enhance this process by providing means to save, copy and load ROIs individually. In texture analysis studies there typically exists some prior knowledge of the analysed subject which indicates the area of interest. Benefits from completely automated segmentation in the ROI selection phase would thus be unlikely and contain high risks.

5.3 Texture features

To confine such an ambitious project it was vital that a limit was introduced already in the requirements stage regarding the features to be implemented. With a focus on GUI design and usability it was natural that by narrowing down to a dozen features including

straightforward adaptation of histogram-based parameters as well as features with higher texture analysis potential such as GLCM and LBP a more realistic scope was achieved.

Implementing the texture features and utilizing the IPT provided access to reliable functionality based on years of excessive testing by the MATLAB community and regularly updated programming code with excellent documentation. Reconstructing every component from the start would have been extremely time-consuming and completely unnecessary. The readily available functionality of the IPT have been optimized in terms of performance and this benefit may be lost in rewriting the code.

The predetermined set of features worked as a reference for comparing and verifying the results from the Visualization module. The histogram-based features were included in this elementary project not only to allow computationally faster analysis in the product testing phase but also to work as a baseline for the whole design and implementation process. GLCM parameters were found to be superior to other available textural features in Chapter 2.2 which was confirmed by the research results involving texture analysis performed with MaZda presented in Chapters 2.4 and 2.5 respectively.

5.4 Texture analysis automation

Due to the high complexity and challenges in repeatability of the image processing steps successful texture analysis automation is yet to achieve an established status in clinical practise. Determining the most significant parameters amongst the huge amount of extracted data using texture analysis has been the main area of focus. As introduced in Chapter 2.2.6 the steps involved in fully automatic texture analysis process are complex. For a method to require several individual medical image processing tools is no rarity. Utilizing the combination of MaZda for texture analysis, OsiriX for ADC estimation and SPSS for statistical analysis was introduced in the parotid gland lesion study discussed in Chapter 2.5.3. Similar example was reported in Chapter 2.5.4 where the ROI selection was carried out in ImageJ and Minitab 15 was used for PCA. Unfortunately these tools are often imaging modality or anatomical region dependent instead of general-purpose and platform independent.

5.5 Suggestions for improvements

Since MATLAB is widely used in education around the world students from medical engineering, software engineering or signal processing backgrounds could provide input in the form of algorithms. With results pending from acceptance testing it is currently recommended to hold further development. Complementing the image processing frame of ImageAnalyzer is suggested to continue with the implementation of elliptic ROI drawing style. Similar to the *imrect* function available in the IPT, applying a function called *imellipse* may be utilized with mapping adjustments made to match 3D space. With several open-source medical image processing software already providing some

level of extendibility it is suggested that the possibility of utilizing the available plugins implemented in C or C++ should be further investigated. Exchanging knowledge regarding MaZda extensions is recommended by contacting members of developer team lead by Professor Materka.

The comparative studies between healthy and pathological tissue presented in Chapter 3 showed that texture analysis succeeded in discriminating the tissues more accurately than using visual analysis by the radiologists in all of the cases. This proves the increasing need to develop general-purpose quantitative texture analysis software primarily for MRI, but to other imaging modalities alike. Focus on the usability and work flow accompanied with effortless extensibility and configuration can provide support for the diagnosis and even results that can ultimately be integrated to clinical practice.

6 CONCLUSIONS

Medical image processing software applications of all purposes are faced with continuous increasing demands of information technology evolving faster than the actual image acquisition methods. Whereas the next generation imaging modality is required to undergo a wide range of certifications and acceptance tests by various authorities, the image processing field is much further ahead. Promising open-source applications have been developed for medical image post-processing of great mathematical complexity but creating a diagnostically efficient multipurpose tool is yet to take place.

In this thesis open-source software for medical image processing was discovered diverse and function-driven without common tools for more generic approach. This is explained by the various standards present in the healthcare sector but also by the lack of unique guidelines for software development in medical informatics.

Using texture analysis for classification of pathological and healthy tissue in MR images is a promising image processing method for medical images. However, current diagnostic applications suffer from the complicated image acquisition process involved in the sophisticated MRI process. This complexity is currently affecting also the computational analysis steps such as texture analysis. Clinically significant results in image analysis would require increased spatial resolution and homogenous imaging conditions. Several imaging occasions can be required even years apart. Patient-related problems like involuntary movement cannot be removed altogether but means to reduce and minimize these type of artefacts are constantly promoted.

The results of texture analysis research on MR images using MaZda software was discovered to have diagnostic potential on most of the studies. Unfortunately competing applications were not found for more detailed comparison of the performance and functionality. In some cases the unsatisfactory detection or classification cases involved challenges related to the image data itself rather than explicitly on software deficiency. Unfortunately the image acquisition can rarely be redone but adjusting the texture analysis application accordingly is rather simple.

For the use of the texture analysis group at TAUH a custom MATLAB application was implemented to create an extensible platform for highly modifiable and compact purposes of textural analysis of MR image data. The design and implementation process was inspired by the MaZda texture analysis tool. Coupled with the experience in utilizing texture parameters in MR image data analysis the objective was to channel the detected areas of improvements into a competent software. Modular application structure and redesigned GUI enabled intuitive interaction through multiple image series

during a single session. Removing the ROI number limitation and switching to 2D drawing of the ROI allowed more precise control for the user. Cubical ROI draw style was implemented to give reference of the feature parameters. Elliptic ROI drawing style is suggested as the next step in development as well as an improved 3D visualization with ROIs included. The total flow of texture analysis from loading the images to feature extraction to Excel format was also improved. The co-occurrence matrix in 3D and the LBP features were embedded using available solutions.

Even though only a fraction of the features present in MaZda were implemented the objective of creating a user friendly, compact and fully customisable frame was achieved. Further testing by the end users in research, additional development of features and result comparison with MaZda is required to complement the tool.

REFERENCES

[1] Julesz, B. & Bergen, J.R. Human Factors and Behavioral Science: Textons, The Fundamental Elements in Preattentive Vision and Perception of Textures. Bell System Technical Journal 62(1983)6, pp. 1619-1645.

[2] Szczypinski, P.M., Strzelecki, M. & Materka, A. Mazda - a software for texture analysis. International Symposium on Information Technology Convergence, 2007, pp. 245-249.

[3] Hornak, J.P. The Basics of MRI. Interactive Learning Software. Henietta, New York, [Accessed May 2014]. Available at: http://www.cis.rit.edu/htbooks/mri/.

[4] Damadian, R. Tumor detection by nuclear magnetic resonance. Science (New York, N.Y.) 171(1971)3976, pp. 1151-1153.

[5] Hajek, M., Dezortova, M., Materka, A. & Lerski, R. Texture analysis for magnetic resonance imaging. Prague 2006, Med4publishing.

[6] Huettel, S.A., Song, A.W. & McCarthy, G. Functional magnetic resonance imaging. 2004, Sinauer Associates Sunderland, MA.

[7] Guo, Y., Cai, Y.Q., Cai, Z.L., Gao, Y.G., An, N.Y., Ma, L., Mahankali, S. & Gao, J.H. Differentiation of clinically benign and malignant breast lesions using diffusion-weighted imaging. Journal of magnetic resonance imaging : JMRI 16(2002)2, pp. 172-178.

[8] Mori, S. & Zhang, J. Diffusion Tensor Imaging (DTI). In: Squire, L.R. (ed.). Encyclopedia of Neuroscience. Oxford 2009, Academic Press. pp. 531-538.

[9] Chen, W., Giger, M.L., Li, H., Bick, U. & Newstead, G.M. Volumetric texture analysis of breast lesions on contrast-enhanced magnetic resonance images. Magnetic resonance in medicine : official journal of the Society of Magnetic Resonance in Medicine / Society of Magnetic Resonance in Medicine 58(2007)3, pp. 562-571.

[10] Doan, N.T., van den Bogaard, S.J., Dumas, E.M., Webb, A.G., van Buchem, M.A., Roos, R.A., van der Grond, J., Reiber, J.H. & Milles, J. Texture analysis of ultrahigh field T2*-weighted MR images of the brain: application to Huntington's disease. Journal of magnetic resonance imaging : JMRI 39(2014)3, pp. 633-640.

[11] van der Graaf, M. In vivo magnetic resonance spectroscopy: basic methodology and clinical applications. European biophysics journal : EBJ 39(2010)4, pp. 527-540.

[12] Kaizer, H. A quantification of textures on aerial photographs. Boston University Research Laboratory 1955, Technical Note 121, AD 69484.

[13] Haralick, R.M., Shanmugam, K. & Dinstein, I. Textural Features for Image Classification. IEEE Transactions on Systems, Man and Cybernetics SMC-3(1973)6, pp. 610-621.

[14] Castellano, G., Bonilha, L., Li, L. & Cendes, F. Texture analysis of medical images. Clinical radiology 59(2004)12, pp. 1061-1069.

[15] Haralick, R.M. Statistical and structural approaches to texture. Proceedings of the IEEE 67(1979)5, pp. 786-804.

[16] Qian, S. & Chen, D. Discrete Gabor transform. IEEE Transactions on Signal Processing 41(1993)7, pp. 2429-2438.

[17] Graps, A. An introduction to wavelets. IEEE Computational Science & Engineering 2(1995)2, pp. 50-61.

[18] Livens, S., Scheunders, P., Van de Wouwer, G. & Van Dyck, D. Wavelets for texture analysis, an overview. Sixth International Conference on Image Processing and Its Applications, Jul 14. 1997, IET. pp. 581-585.

[19] He, D. & Wang, L. Texture Unit, Texture Spectrum And Texture Analysis. Geoscience and Remote Sensing Symposium. IGARSS'89. 12th Canadian Symposium on Remote Sensing. Jul 14. 1989, IEEE. pp. 2769-2772.

[20] Wang, L. & He, D. Texture classification using texture spectrum. Pattern Recognition 23(1990)8, pp. 905-910.

[21] Ojala, T., Pietikainen, M. & Harwood, D. Performance evaluation of texture measures with classification based on Kullback discrimination of distributions. Proceedings of the 12th IAPR International Conference on Pattern Recognition. Vol. 1 - Conference A: Computer Vision & Image Processing. 9 - 13 Oct. 1994, IEEE. pp. 582-585.

[22] Harwood, D., Ojala, T., Pietikainen, M., Kelman, S. & Davis, L. Texture classification by center-symmetric auto-correlation, using Kullback discrimination of distributions. Pattern Recognition Letters 16(1995)1, pp. 1-10.

[23] Ojala, T., Pietikainen, M. & Harwood, D. A comparative study of texture measures with classification based on featured distributions. Pattern Recognition 29(1996)1, pp. 51-59.

[24] Ojala, T., Pietikainen, M. & Maenpaa, T. Gray scale and rotation invariant texture classification with local binary patterns. In: Vernon, D. (ed.). Computer Vision - ECCV 2000. 2000, Springer. pp. 404-420.

[25] Ojala, T., Pietikainen, M. & Maenpaa, T. A generalized local binary pattern operator for multiresolution gray scale and rotation invariant texture classification. In: Singh, S., Murshed, N. & Kropatsch, W. (ed.). Advances in Pattern Recognition - ICAPR 2001. 2001, Springer. pp. 399-408.

[26] Ojala, T., Pietikainen, M. & Maenpaa, T. Multiresolution gray-scale and rotation invariant texture classification with local binary patterns. IEEE Transactions on Pattern Analysis and Machine Intelligence 24(2002)7, pp. 971-987.

[27] Ahonen, T., Hadid, A. & Pietikainen, M. Face Recognition with Local Binary Patterns. In: Pajdla, T. & Matas, J. (ed.). Computer Vision - ECCV 2004. 2004, Springer. pp. 469-481.

[28] Ahonen, T., Hadid, A. & Pietikainen, M. Face Description with Local Binary Patterns: Application to Face Recognition. IEEE Transactions on Pattern Analysis and Machine Intelligence 28(2006)12, pp. 2037-2041.

[29] Zhou, H., Wang, R. & Wang, C. A novel extended local-binary-pattern operator for texture analysis. Information Sciences 178(2008)22, pp. 4314-4325.

[30] Fathi, A. & Naghsh-Nilchi, A.R. Noise tolerant local binary pattern operator for efficient texture analysis. Pattern Recognition Letters 33(2012)9, pp. 1093-1100.

[31] Fehr, J. & Burkhardt, H. 3D rotation invariant local binary patterns. ICPR, 2008, Citeseer. pp. 1-4.

[32] Unay, D., Ekin, A., Cetin, M., Jasinschi, R. & Ercil, A. Robustness of Local Binary Patterns in Brain MR Image Analysis. Engineering in Medicine and Biology Society, 2007. EMBS 2007. 29th Annual International Conference of the IEEE, 2007, pp. 2098-2101.

[33] Unay, D. & Ekin, A. Intensity versus texture for medical image search and retrival. 5th IEEE International Symposium on Biomedical Imaging: From Nano to Macro. 2008, ISBI. pp. 241-244.

[34] Zhou, Z., Liu, W., Cui, J., Wang, X., Arias, D., Wen, Y., Bansal, R., Hao, X., Wang, Z., Peterson, B.S. & Xu, D. Automated artifact detection and removal for improved tensor estimation in motion-corrupted DTI data sets using the combination of local binary patterns and 2D partial least squares. Magnetic resonance imaging 29(2011)2, pp. 230-242.

[35] Ibanez, L., Schroeder, W., Ng, L. & Cates, J. The ITK Software Guide. 2003, Kitware, Inc.

[36] Yushkevich, P.A., Piven, J., Hazlett, H.C., Smith, R.G., Ho, S., Gee, J.C. & Gerig, G. User-guided 3D active contour segmentation of anatomical structures: significantly improved efficiency and reliability. NeuroImage 31(2006)3, pp. 1116-1128.

[37] Wolf, I., Vetter, M., Wegner, I., Böttger, T., Nolden, M., Schöbinger, M., Hastenteufel, M., Kunert, T. & Meinzer, H. The Medical Imaging Interaction Toolkit. Medical image analysis 9(2005)6, pp. 594-604.

[38] Fedorov, A., Beichel, R., Kalpathy-Cramer, J., Finet, J., Fillion-Robin, J., Pujol, S., Bauer, C., Jennings, D., Fennessy, F., Sonka, M., Buatti, J., Aylward, S., Miller, J.V., Pieper, S. & Kikinis, R. 3D Slicer as an image computing platform for the Quantitative Imaging Network. Magnetic resonance imaging 30(2012)9, pp. 1323-1341.

[39] Schneider, C.A., Rasband, W.S. & Eliceiri, K.W. NIH Image to ImageJ: 25 years of image analysis. Nature methods 9(2012)7, pp. 671-675.

[40] McAuliffe, M.J., Lalonde, F.M., McGarry, D., Gandler, W., Csaky, K. & Trus, B.L. Medical image processing, analysis and visualization in clinical research. 4th IEEE Symposium on Computer-Based Medical Systems, 2001, IEEE. pp. 381-386.

[41] MIPAV Documentation. National Institutes of Health. Center for Information Technology, Bethesda, Maryland, [Accessed May 2014]. Available at: http://mipav.cit.nih.gov/pubwiki/index.php/MIPAV_Help.

[42] Szczypinski, P.M., Strzelecki, M. & Materka, A. Mazda - a software for texture analysis. International Symposium on Information Technology Convergence, 2007, pp. 245-249.

[43] Strzelecki, M., Szczypinski, P., Materka, A. & Klepaczko, A. A software tool for automatic classification and segmentation of 2D/3D medical images. Nuclear Instruments and Methods in Physics Research Section A: Accelerators, Spectrometers, Detectors and Associated Equipment 702(2013) pp. 137-140.

[44] Szczypiński, P.M., Strzelecki, M., Materka, A. & Klepaczko, A. MaZda—A software package for image texture analysis. Computer methods and programs in biomedicine 94(2009)1, pp. 66-76.

[45] Herlidou, S., Rolland, Y., Bansard, J.Y., Le Rumeur, E. & de Certaines, J.D. Comparison of automated and visual texture analysis in MRI: Characterization of normal and diseased skeletal muscle. Magnetic resonance imaging 17(1999)9, pp. 1393-1397.

[46] Harrison, L., Dastidar, P., Eskola, H., Jarvenpaa, R., Pertovaara, H., Luukkaala, T., Kellokumpu-Lehtinen, P.L. & Soimakallio, S. Texture analysis on MRI images of non-Hodgkin lymphoma. Computers in biology and medicine 38(2008)4, pp. 519-524.

[47] Harrison, L.C., Luukkaala, T., Pertovaara, H., Saarinen, T.O., Heinonen, T.T., Jarvenpaa, R., Soimakallio, S., Kellokumpu-Lehtinen, P.L., Eskola, H.J. & Dastidar, P. Non-Hodgkin lymphoma response evaluation with MRI texture classification. Journal of experimental & clinical cancer research : CR 28(2009) pp. 87.

[48] Savio, S.J., Harrison, L.C., Luukkaala, T., Heinonen, T., Dastidar, P., Soimakallio, S. & Eskola, H.J. Effect of slice thickness on brain magnetic resonance image texture analysis. Biomedical engineering online 9(2010)60, pp. 1-14.

[49] Harrison, L.C., Nikander, R., Sikio, M., Luukkaala, T., Helminen, M.T., Ryymin, P., Soimakallio, S., Eskola, H.J., Dastidar, P. & Sievanen, H. MRI texture analysis of femoral neck: Detection of exercise load-associated differences in trabecular bone. Journal of magnetic resonance imaging : JMRI 34(2011)6, pp. 1359-1366.

[50] Holli, K.K., Harrison, L., Dastidar, P., Waljas, M., Liimatainen, S., Luukkaala, T., Ohman, J., Soimakallio, S. & Eskola, H. Texture analysis of MR images of patients with mild traumatic brain injury. BMC medical imaging 10(2010)8, pp. 1-10.

[51] Holli, K.K., Waljas, M., Harrison, L., Liimatainen, S., Luukkaala, T., Ryymin, P., Eskola, H., Soimakallio, S., Ohman, J. & Dastidar, P. Mild traumatic brain injury: tissue texture analysis correlated to neuropsychological and DTI findings. Academic Radiology 17(2010)9, pp. 1096-1102.

[52] Holli, K., Laaperi, A.L., Harrison, L., Luukkaala, T., Toivonen, T., Ryymin, P., Dastidar, P., Soimakallio, S. & Eskola, H. Characterization of breast cancer types by texture analysis of magnetic resonance images. Academic Radiology 17(2010)2, pp. 135-141.

[53] Sikio, M., Holli, K.K., Harrison, L.C., Ruottinen, H., Rossi, M., Helminen, M.T., Ryymin, P., Paalavuo, R., Soimakallio, S., Eskola, H.J., Elovaara, I. & Dastidar, P. Parkinson's disease: interhemispheric textural differences in MR images. Academic Radiology 18(2011)10, pp. 1217-1224.

[54] Sikio, M., Holli-Helenius, K.K., Harrison, L.C., Ryymin, P., Ruottinen, H., Saunamaki, T., Eskola, H.J., Elovaara, I. & Dastidar, P. MR image texture in Parkinson's disease: a longitudinal study. Acta Radiologica (Stockholm, Sweden : 1987) (2014).

[55] Zhang, J., Yu, C., Jiang, G., Liu, W. & Tong, L. 3D texture analysis on MRI images of Alzheimer's disease. Brain imaging and behavior 6(2012)1, pp. 61-69.

[56] de Oliveira, M.S., Betting, L.E., Mory, S.B., Cendes, F. & Castellano, G. Texture analysis of magnetic resonance images of patients with juvenile myoclonic epilepsy. Epilepsy & Behavior 27(2013)1, pp. 22-28.

[57] Jimenez del Toro, O.A., Foncubierta-Rodriguez, A., Vargas Gomez, M.I., Muller, H. & Depeursinge, A. Epileptogenic lesion quantification in MRI using contralateral 3D texture comparisons. International Conference on Medical Image Computing and Computer-Assisted Intervention 16(2013)2, pp. 353-360.

[58] Fruehwald-Pallamar, J., Czerny, C., Holzer-Fruehwald, L., Nemec, S.F., Mueller-Mang, C., Weber, M. & Mayerhoefer, M.E. Texture-based and diffusion-weighted discrimination of parotid gland lesions on MR images at 3.0 Tesla. NMR in biomedicine 26(2013)11, pp. 1372-1379.

[59] Levy, A.S. Brain Tumors in Children: Evaluation and Management. Current Problems in Pediatric and Adolescent Health Care 35(2005)6, pp. 230-245.

[60] Orphanidou-Vlachou, E., Vlachos, N., Davies, N.P., Arvanitis, T.N., Grundy, R.G. & Peet, A.C. Texture analysis of T1 - and T2 -weighted MR images and use of probabilistic neural network to discriminate posterior fossa tumours in children. NMR in biomedicine 27(2014)6, pp. 632-639.

[61] Hammond, W.E. & Cimino, J.J. Standards in medical informatics. In: Shortliffe, E.H. & Perreault, L.E. (ed.). Medical Informatics - Computer Applications in Health Care and Biomedicine. 2001, Springer. pp. 212-256.

[62] Issler, L., Spreckelsen, C. & Wessel, C. Implementing software development guidelines in a medical informatics research project. Methods of information in medicine 46(2007)6, pp. 641-645.

[63] IEEE Standard Glossary of Software Engineering Terminology. ANSI/IEEE Standard 610.12-1990. 1990, Institute of Electrical and Electronics Engineers.

[64] ISO/IEC 25010:2011 Systems and software engineering - Systems and software Quality Requirements and Evaluation (SQuaRE) - System and software quality models. 2011, International Organization for Standardization.

[65] MATLAB Documentation. The MathWorks, Inc. [Accessed May 2014]. Available at: http://www.mathworks.se/help/matlab/index.html.

[66] MATLAB and Image Processing Toolbox Release 2013a. Natick, Massachusetts, United States. The MathWorks, Inc.

[67] Heikkila, M. & Ahonen, T. LBP Implementation in MATLAB. Department of Computer Science and Engineering, University of Oulu, 2000, [Accessed May 2014]. Available at: http://www.cse.oulu.fi/CMV/Downloads/LBPMatlab.

[68] Philips, C. & Li, D. Implementation of 3D co-occurrence matrix and Haralick features in MATLAB. MATLAB Central, March 2008, [Accessed May 2014]. Available at: http://www.mathworks.com/matlabcentral/fileexchange/19058-cooc3d.

APPENDIX 1: IMAGEANALYZER USER INTERFACE LAYOUT